The $D(D_3)$-anyon chain: integrable boundary conditions and excitation spectra

2013 New J. Phys. 15 053035

(http://iopscience.iop.org/1367-2630/15/5/053035)

New Journal of Physics
The open access journal for physics

The $D(D_3)$-anyon chain: integrable boundary conditions and excitation spectra

Peter E Finch and Holger Frahm[1]
Institut für Theoretische Physik, Leibniz Universität Hannover, Appelstraße 2, D-30167 Hannover, Germany
E-mail: frahm@itp.uni-hannover.de

New Journal of Physics **15** (2013) 053035 (33pp)
Received 20 November 2012
Published 22 May 2013
Online at http://www.njp.org/
doi:10.1088/1367-2630/15/5/053035

Abstract. Chains of interacting non-Abelian anyons with local interactions invariant under the action of the Drinfeld double of the dihedral group D_3 are constructed. Formulated as a spin chain the Hamiltonians are generated from commuting transfer matrices of an integrable vertex model for periodic and braided as well as open boundaries. A different anyonic model with the same local Hamiltonian is obtained within the fusion path formulation. This model is shown to be related to an integrable fusion interaction round the face model. Bulk and surface properties of the anyon chain are computed from the Bethe equations for the spin chain. The low-energy effective theories and operator content of the models (in both the spin chain and fusion path formulation) are identified from analytical and numerical studies of the finite-size spectra. For all boundary conditions considered the continuum theory is found to be a product of two conformal field theories. Depending on the coupling constants the factors can be a Z_4 parafermion or a $\mathcal{M}_{(5,6)}$ minimal model.

[1] Author to whom any correspondence should be addressed.

Contents

1. Introduction

In recent years there has been a surge of attention directed towards the understanding of many-particle systems exhibiting topological order, i.e. phases that cannot be characterized by a local order parameter. Possible realizations of such topological quantum liquids in condensed matter physics are the fractional quantum Hall (FQH) states [44, 50] and certain two-dimensional frustrated quantum magnets [6, 39, 49]. The excitations in these systems display anyonic statistics and an understanding of their collective behaviour is essential for the classification of topological phase transitions. Particularly interesting are non-Abelian anyons where the interchange of two particles is described by non-trivial representations of the braid group complemented by fusion rules for the decomposition of product states. The fact that these non-Abelian anyons are protected by their topological charge has led to proposals for the use of such systems in universal quantum computation [40, 51].

Some insight into the peculiar properties of many interacting anyons can be obtained in the context of simple model systems: such models can be obtained by associating anyonic degrees of freedom with each site of a lattice and defining interactions compatible with their braiding and fusion rules [20]. The phase diagram of the resulting lattice models can be studied based on the numerical computation of finite-size spectra. This approach is particularly powerful for anyonic chains, i.e. one-dimensional lattices, where the numerical data can be compared against predictions from conformal field theory (CFT). Another approach, also in one dimension, makes use of the fact that the lattice model may become integrable for particular choices of coupling constants. For the solution of such models, various analytical methods, e.g. in the framework

of the quantum inverse scattering method (QISM), have been established which allow the study of the spectrum of their low-energy excitations, their thermodynamical properties including the long-distance asymptotics of correlation functions and even form factors [41, 42].

So far much of the work on such lattice models has been focused on systems of the non-Abelian Ising or Fibonacci anyons related to the quasi-particles in certain FQH states and their generalizations appearing in $su(2)_k$ Chern–Simons theories [5, 20, 31, 45, 59, 60]. These anyons have relatively simple fusion rules which allows for tractable computation of systems with nearest and next-nearest-neighbour interactions. Integrable points within the one-dimensional versions of these models have been identified as restricted solid-on-solid (RSOS) or interaction round the face (IRF) models constructed from representations of Temperley–Lieb algebras [20, 36, 37]. An alternative method to define an anyonic theory is via the Drinfeld doubles of a finite group algebra, $D(G)$, and its representations [15]. The quasi-particles in these systems are irreducible representations (irreps) of $D(G)$ labelled by their flux, i.e. an element of $h \in G$, and their topological charge determined by the transformation properties under the residual global symmetry commuting with the flux h.

Being a quasi-triangular Hopf algebra with a Baxterised R-matrix, the quantum double allows for a direct construction of integrable quantum chains with nearest-neighbour interactions described by a local Hamiltonian which is invariant under the corresponding symmetry [14, 21]: within the QISM one obtains quantum spin chains on a Hilbert space being a tensor product of the finite-dimensional local spaces corresponding to a spin S, a qudit or a more general n-state quantum system. On the other hand, it is already known that for any given model whose local Hamiltonian has the symmetry of a quasi-triangular Hopf algebra associated with an anyonic theory, it is possible to construct quantum chains using the fusion path formalism [22]. Here the basis vectors are composed of sequences of anyons and we shall refer to this as a fusion path chain. The local Hamiltonian is formally identical in the spin and the fusion path formalism. Therefore, one should expect the bulk properties of the spin and the fusion path model to be the same. The finite-size spectrum of low-energy excitations, however, is known to depend on boundary conditions [4, 11] and therefore should differ between the two realizations.

In this paper we study this problem for a specific one-dimensional anyon chain with nearest-neighbour interactions. The underlying symmetry of the Hamiltonian is that of the Drinfeld double of a dihedral group, specifically $D(D_3)$. In the following section, we define this algebra and recall its irreps and the corresponding fusion rules. Then, using the spin basis, integrable models are constructed subject to periodic, braided and open boundary conditions, all of which being based on the usual QISM transfer matrix [24]. While for the fusion path basis we construct a fusion IRF transfer matrix whose series expansion contains the global one-dimensional Hamiltonian. In section 3 we compute the bulk and surface properties of the model from the Bethe ansatz formulation of the spectral properties for the spin chain. The CFT and operator content for the periodic spin chain version of the $D(D_3)$ model has been identified previously [23]. In section 4 we expand this work providing more details on the analysis as well as extending the study of the finite-size spectrum to the spin chain with braided and open boundary conditions. In addition, we present results for the fusion path chain in support of the expectation that the low-energy excitations of the $D(D_3)$-anyon chain are described by the same CFT for all types of boundary conditions studied here, namely products of Z_4 parermion and $\mathcal{M}_{(5,6)}$ minimal models.

2. The model and its symmetries

2.1. The $D(D_3)$ algebra

The model we consider in this paper has the underlying symmetry of the Drinfeld (or quantum) double of a finite group algebra. The finite group we utilize is the dihedral group of order six, D_3, and is isomorphic to the group of permutations on three elements, S_3. This group is based upon the symmetries of an equilateral triangle and has the presentation

$$D_3 = \{\sigma, \tau | \sigma^3 = \tau^2 = \sigma\tau\sigma\tau = e\},$$

where e is the identity element of the group, σ is a rotation and τ is a flip. The Drinfeld double of this group is defined as the vector space

$$D(D_3) = \mathbb{C}\{gh^* | g, h \in D_3\},$$

where $*$ denotes an element from the dual space of $\mathbb{C}D_3$. This space forms a quasi-triangular Hopf algebra when equipped with the multiplication and coproduct,

$$g_1h_1^*g_2h_2^* = \delta_{(h_1g_2)}^{(g_2h_2)}\ (g_1g_2)h_2^* \quad \text{and} \quad \Delta(gh^*) = \sum_{k\in D_3} g(k^{-1}h)^* \otimes gk^*.$$

The remaining structure is uniquely determined by these relations [12, 46]. This algebra has an associated universal R-matrix i.e. an algebraic solution to the Yang–Baxter equation.

2.1.1. Representations. The representation theory of the Drinfeld doubles of finite group algebras are well known [17, 33]. The irreps of $D(D_3)$ are classified by the conjugacy classes of D_3. For a given conjugacy class, a representative element is chosen and the representations of the centralizer subgroup of this element are determined. An action on conjugacy class is defined and then combined in prescribed manner with an irrep of the centralizer. This yields an irrep of $D(D_3)$ labelled by both the representative element and the irrep of the centralizer. The irreps associated with the conjugacy class $\{e\}$ are:

$$\pi^{(e,\pm)}(\sigma) = 1, \qquad \pi^{(e,\pm)}(\tau) = \pm 1, \qquad \pi^{(e,\pm)}(g^*) = \delta_g^e,$$

$$\pi^{(e,1)}(\sigma) = \begin{pmatrix} \omega 0 & \\ 0 & \omega^{-1} \end{pmatrix}, \qquad \pi^{(e,1)}(\tau) = \begin{pmatrix} 0 & 1 \\ 1 & 0 \end{pmatrix}, \qquad \pi^{(e,1)}(g^*) = \begin{pmatrix} \delta_g^e & 0 \\ 0 & \delta_g^e \end{pmatrix},$$

where $\omega = \mathrm{e}^{\frac{2i\pi}{3}}$. The irreps associated with the conjugacy class $\{\sigma, \sigma^2\}$ are:

$$\pi^{(\sigma,k)}(\sigma) = \begin{pmatrix} \omega^k & 0 \\ 0 & \omega^{-k} \end{pmatrix}, \quad \pi^{(\sigma,k)}(\tau) = \begin{pmatrix} 0 & 1 \\ 1 & 0 \end{pmatrix}, \quad \pi^{(\sigma,k)}(g^*) = \begin{pmatrix} \delta_g^\sigma & 0 \\ 0 & \delta_g^{\sigma^2} \end{pmatrix},$$

where $k \in \{0, 1, 2\}$. The irreps associated with the conjugacy class $\{\tau, \sigma\tau, \sigma^2\tau\}$ are:

$$\pi^{(\tau,\pm)}(\sigma) = \begin{pmatrix} 0 & 0 & 1 \\ 1 & 0 & 0 \\ 0 & 1 & 0 \end{pmatrix}, \quad \pi^{(\tau,\pm)}(\tau) = \pm \begin{pmatrix} 1 & 0 & 0 \\ 0 & 0 & 1 \\ 0 & 1 & 0 \end{pmatrix}, \quad \pi^{(\tau,\pm)}(g^*) = \begin{pmatrix} \delta_g^\tau & 0 & 0 \\ 0 & \delta_g^{\sigma^2\tau} & 0 \\ 0 & 0 & \delta_g^{\sigma\tau} \end{pmatrix}.$$

The anyonic theory corresponding with $D(D_3)$ associates an irrep with an anyon [15]. For convenience, it is simpler to denote each irreps by a single letter, $\mathfrak{a}, \ldots, \mathfrak{h}$. We equate

$$\mathfrak{a} = (e, +),\ \mathfrak{b} = (e, -),\ \mathfrak{c} = (e, 1),\ \mathfrak{d} = (\sigma, 0),\ \mathfrak{e} = (\sigma, 1),\ \mathfrak{f} = (\sigma, 2),\ \mathfrak{g} = (\tau, +),\ \mathfrak{h} = (\tau, -).$$

Properties of the anyons are inherited from their associated irreps, e.g. the dimension of an anyon equals the dimension of its corresponding irrep.

2.1.2. Fusion rules. Required for an anyonic theory are the fusion rules of particles. These rules are defined by the tensor product decompositions of the associated irreps [33]:

$$\pi^{\alpha} \otimes \pi^{\beta} = \bigoplus_{\gamma} N_{\alpha\beta}^{\gamma} \pi^{\gamma}, \quad \text{where } N_{\alpha\beta}^{\gamma} = \frac{1}{6} \sum_{g,h,k} \text{tr}\,[\pi^{\alpha}(h^* g^{-1})]\,\text{tr}\,[\pi^{\beta}(g(k^{-1}h)^*)]\,\text{tr}\,[\pi^{\gamma}(gk^*)]$$

and tr is the trace. Applying the above formula yields the following fusion rules presented in terms of the associated labels:

$\otimes$	$\mathfrak{a}$	$\mathfrak{b}$	$\mathfrak{c}$	$\mathfrak{d}$	$\mathfrak{e}$	$\mathfrak{f}$	$\mathfrak{g}$	$\mathfrak{h}$
$\mathfrak{a}$	$\mathfrak{a}$	$\mathfrak{b}$	$\mathfrak{c}$	$\mathfrak{d}$	$\mathfrak{e}$	$\mathfrak{f}$	$\mathfrak{g}$	$\mathfrak{h}$
$\mathfrak{b}$	$\mathfrak{b}$	$\mathfrak{a}$	$\mathfrak{c}$	$\mathfrak{d}$	$\mathfrak{e}$	$\mathfrak{f}$	$\mathfrak{h}$	$\mathfrak{g}$
$\mathfrak{c}$	$\mathfrak{c}$	$\mathfrak{c}$	$\mathfrak{a}\oplus\mathfrak{b}\oplus\mathfrak{c}$	$\mathfrak{e}\oplus\mathfrak{f}$	$\mathfrak{d}\oplus\mathfrak{f}$	$\mathfrak{d}\oplus\mathfrak{e}$	$\mathfrak{g}\oplus\mathfrak{h}$	$\mathfrak{g}\oplus\mathfrak{h}$
$\mathfrak{d}$	$\mathfrak{d}$	$\mathfrak{d}$	$\mathfrak{e}\oplus\mathfrak{f}$	$\mathfrak{a}\oplus\mathfrak{b}\oplus\mathfrak{d}$	$\mathfrak{c}\oplus\mathfrak{f}$	$\mathfrak{c}\oplus\mathfrak{e}$	$\mathfrak{g}\oplus\mathfrak{h}$	$\mathfrak{g}\oplus\mathfrak{h}$
$\mathfrak{e}$	$\mathfrak{e}$	$\mathfrak{e}$	$\mathfrak{d}\oplus\mathfrak{f}$	$\mathfrak{c}\oplus\mathfrak{f}$	$\mathfrak{a}\oplus\mathfrak{b}\oplus\mathfrak{e}$	$\mathfrak{c}\oplus\mathfrak{d}$	$\mathfrak{g}\oplus\mathfrak{h}$	$\mathfrak{g}\oplus\mathfrak{h}$
$\mathfrak{f}$	$\mathfrak{f}$	$\mathfrak{f}$	$\mathfrak{d}\oplus\mathfrak{e}$	$\mathfrak{c}\oplus\mathfrak{e}$	$\mathfrak{c}\oplus\mathfrak{d}$	$\mathfrak{a}\oplus\mathfrak{b}\oplus\mathfrak{f}$	$\mathfrak{g}\oplus\mathfrak{h}$	$\mathfrak{g}\oplus\mathfrak{h}$
$\mathfrak{g}$	$\mathfrak{g}$	$\mathfrak{h}$	$\mathfrak{g}\oplus\mathfrak{h}$	$\mathfrak{g}\oplus\mathfrak{h}$	$\mathfrak{g}\oplus\mathfrak{h}$	$\mathfrak{g}\oplus\mathfrak{h}$	$\mathfrak{a}\oplus\mathfrak{c}\oplus\mathfrak{d}\oplus\mathfrak{e}\oplus\mathfrak{f}$	$\mathfrak{b}\oplus\mathfrak{c}\oplus\mathfrak{d}\oplus\mathfrak{e}\oplus\mathfrak{f}$
$\mathfrak{h}$	$\mathfrak{h}$	$\mathfrak{g}$	$\mathfrak{g}\oplus\mathfrak{h}$	$\mathfrak{g}\oplus\mathfrak{h}$	$\mathfrak{g}\oplus\mathfrak{h}$	$\mathfrak{g}\oplus\mathfrak{h}$	$\mathfrak{b}\oplus\mathfrak{c}\oplus\mathfrak{d}\oplus\mathfrak{e}\oplus\mathfrak{f}$	$\mathfrak{a}\oplus\mathfrak{c}\oplus\mathfrak{d}\oplus\mathfrak{e}\oplus\mathfrak{f}$

2.2. Local spin Hamiltonians

The $D(D_3)$ model is constructed by taking a special case of the three-state Fateev–Zamolodchikov model [19]. This limit yields the R-matrix, which can also be constructed from the $\pi^{\mathfrak{g}} \otimes \pi^{\mathfrak{g}}$ representation of $D(D_3)$ [21],

$$R(z_1, z_2) = N(z_1, z_2) \sum_{a,b,i,j=0}^{2} \left[w^{(i-j)(a-b)} \overline{W}(z_1|a) \overline{W}(z_2^{-1}|b) \right] e_{i+a+b,i} \otimes e_{j+a+b,j}, \tag{1}$$

where $e_{i,j}$ represents a 3×3 matrix (whose indices are considered modulo three) with a one in the ith row and jth column and zeros elsewhere,

$$\overline{W}(z|l) = \left[\frac{z-1}{wz - w^2} \right]^{1-\delta_l^0} \quad \text{and} \quad N(z_1, z_2) = -\frac{1}{3}(wz_1 - w^2)(w - w^2 z_2).$$

The R-matrix satisfies a Yang–Baxter equation in *both* the first and the second spectral parameters

$$R_{12}(x_1, x_2) R_{23}(x_1 y_1, x_2 y_2) R_{12}(y_1, y_2) = R_{23}(y_1, y_2) R_{12}(x_1 y_1, x_2 y_2) R_{23}(x_1, x_2), \tag{2}$$

and has the symmetry of $D(D_3)$, implying that the operator can be expressed in terms of projection operators. The projection operators from $\pi_{\mathfrak{g}} \otimes \pi_{\mathfrak{g}}$ to the irreps in its decomposition are

$$p^{(a)} = \frac{\dim(a)}{6} \sum_{g,h} \text{tr}\,[\pi^{a}(h^* g^{-1})](\pi^{\mathfrak{g}} \otimes \pi^{\mathfrak{g}})\Delta(gh^*). \tag{3}$$

In terms of these projection operators, the R-matrix is written as

$$R(z_1, z_2) = f_{\mathfrak{a}}(z_1, z_2) p^{(\mathfrak{a})} + f_{\mathfrak{c}}(z_1, z_2) p^{(\mathfrak{c})} + f_{\mathfrak{d}}(z_1, z_2) p^{(\mathfrak{d})} + f_{\mathfrak{e}}(z_1, z_2) p^{(\mathfrak{e})} + f_{\mathfrak{f}}(z_1, z_2) p^{(\mathfrak{f})}, \tag{4}$$

where

$$f_a(z_1, z_2)\, p^{(a)} = R(z_1, z_2)\, p^{(a)}, \quad a \in \{\mathfrak{a}, \mathfrak{c}, \mathfrak{d}, \mathfrak{e}, \mathfrak{f}\}.$$

This R-matrix allows us to construct integrable models subject to various boundary conditions [24]. In the spin chain formulation each lattice site carries a representation $\pi^{\mathfrak{g}}$ of $D(D_3)$. As a consequence of the dependence of the R-matrix on two spectral parameters, there exist two local Hamiltonians describing the interaction between neighbouring spins in the Hilbert space from $\pi^{\mathfrak{g}} \otimes \pi^{\mathfrak{g}}$ representation. The local Hamiltonians are obtained in the usual manner by taking derivatives of the R-matrix with respect to the spectral parameters:

$$h^{(k)} = \mathrm{i}\, \frac{\mathrm{d}}{\mathrm{d}z_k} R(z_1, z_2)\Big|_{z_1=1, z_2=1} - \beta_k I \otimes I,$$

where $k \in \{1, 2\}$ and $\beta_k \in \mathbb{C}$ is chosen such that the trace of the local Hamiltonians is zero. In terms of the projectors (3) the local Hamiltonians are given by [23]

$$h^{(1)} = \frac{2\sqrt{3}}{3} p^{(\mathfrak{a})} - \frac{\sqrt{3}}{3} p^{(\mathfrak{c})} - \frac{\sqrt{3}}{3} p^{(\mathfrak{d})} - \frac{\sqrt{3}}{3} p^{(\mathfrak{e})} + \frac{2\sqrt{3}}{3} p^{(\mathfrak{f})},$$

$$h^{(2)} = \frac{2\sqrt{3}}{3} p^{(\mathfrak{a})} - \frac{\sqrt{3}}{3} p^{(\mathfrak{c})} - \frac{\sqrt{3}}{3} p^{(\mathfrak{d})} + \frac{2\sqrt{3}}{3} p^{(\mathfrak{e})} - \frac{\sqrt{3}}{3} p^{(\mathfrak{f})}. \tag{5}$$

It follows that the local Hamiltonians commute with each other and with the action of the algebra:

$$\left[h^{(1)}, h^{(2)}\right] = 0 \quad \text{and} \quad \left[(\pi_{\mathfrak{g}} \otimes \pi_{\mathfrak{g}})\Delta(a), h^{(k)}\right] = 0,$$

for all $a \in D(D_3)$. Therefore they have the underlying symmetry of $D(D_3)$ as the R-matrix did. From explicit calculation of $h^{(1)}$ and $h^{(2)}$, we find

$$h^{(1)} = \Pi h^{(2)} \Pi = \left[h^{(2)}\right]^*,$$

where Π is usual two-site permutation operator and $*$ is, and herein reserved for, complex conjugation. Both local Hamiltonians (5) are self-adjoint.

2.3. Global Hamiltonian

In the following we shall consider a variety of models with interactions described by the local operators (5) but subject to different boundary conditions. As a consequence of the existence of two distinct local Hamiltonians, the global Hamiltonian is comprised of two terms weighted by a free coupling parameter $\theta \in [0, 2\pi]$ as

$$\mathcal{H}_\theta = \cos(\theta)\, \mathcal{H}^{(1)} + \sin(\theta)\, \mathcal{H}^{(2)}. \tag{6}$$

For all boundary conditions considered below these models are integrable, thanks to the existence of a commuting transfer matrix. Furthermore, the two components of the global Hamiltonian will commute,

$$\left[\mathcal{H}^{(1)}, \mathcal{H}^{(2)}\right] = 0. \tag{7}$$

This commutativity will be particularly useful in the investigation of the models as it allows us to study the spectra of $\mathcal{H}^{(1)}$ and $\mathcal{H}^{(2)}$ separately. Typically, the spectra of $\mathcal{H}^{(1)}$ and $\mathcal{H}^{(2)}$ will be identical or of a related form.

2.3.1. Periodic spin chain. We begin by considering the $D(D_3)$ model as a spin chain with periodic boundary conditions: its global Hamiltonians are defined by

$$\mathcal{H}^{(k)} = h^{(k)}_{\mathcal{L}0} + \sum_{j=1}^{\mathcal{L}-1} h^{(k)}_{j(j+1)},$$

for $k \in \{1, 2\}$. Note that the periodic closure by the term $h^{(k)}_{\mathcal{L}0}$ in the global Hamiltonian breaks the $D(D_3)$ invariance of the model. Both of these Hamiltonians appear in the series expansion of the commuting transfer matrix

$$t(z_1, z_2) = \mathrm{tr}_0 \left[\Pi_{0\mathcal{L}} R_{0\mathcal{L}}(z_1, z_2^*) \cdots \Pi_{01} R_{01}(z_1, z_2^*)\right].$$

By construction this transfer matrix is a polynomial of degree $\mathcal{L}$ in the variables z_1 and z_2^*. It has been observed that this transfer matrix factorizes and that its eigenvalues are always of the form [24]

$$\Lambda(z_1, z_2) = c \prod_{\ell=1}^{\mathcal{L}} (z_1 - z_{1,\ell}) \prod_{\ell=1}^{\mathcal{L}} (z_2 - z_{2,\ell})^*. \tag{8}$$

Therefore, the eigenvalues can be conveniently described in terms of their zeros $z_{k,\ell} \equiv \mathrm{i}\omega \mathrm{e}^{x_{k,\ell}}$, for $k = 1, 2$ and $\ell = 1, \ldots, \mathcal{L}$. Furthermore, starting from the $D(D_3)$ fusion rules functional relations satisfied by the transfer matrices (or equivalently their eigenvalues) can be derived [21]:

$$\begin{aligned}
&\lambda_1(z_1)\Lambda(z_1, z_2) = (\omega z_1 + 1)^{\mathcal{L}} \Lambda(\omega z_1, z_2) + (z_1 - 1)^{\mathcal{L}} \Lambda(\omega^{-1} z_1, z_2), \\
&\lambda_2(z_2)\,[\Lambda(z_1, z_2)]^* = (\omega z_2 + 1)^{\mathcal{L}}\,[\Lambda(z_1, \omega z_2)]^* + (z_2 - 1)^{\mathcal{L}} \left[\Lambda(z_1, \omega^{-1} z_2))\right]^*,
\end{aligned} \tag{9}$$

where $\lambda_k(z)$ are analytic functions. This implies that the two sets of parameters $\{x_{k,\ell}\}_{\ell=1}^{\mathcal{L}}$ must independently satisfy the Bethe equations [24]

$$(-1)^{\mathcal{L}+1} \left(\frac{1 + (\mathrm{i}/\omega)\mathrm{e}^{x_{k,j}}}{1 - \mathrm{i}\omega\, \mathrm{e}^{x_{k,j}}}\right)^{\mathcal{L}} = \prod_{l=1}^{\mathcal{L}} \frac{\mathrm{e}^{x_{k,l}} - (1/\omega)\mathrm{e}^{x_{k,j}}}{\mathrm{e}^{x_{k,l}} - \omega\, \mathrm{e}^{x_{k,j}}}, \quad j = 1, \ldots, \mathcal{L}. \tag{10}$$

It is important to note that while there are exactly $\mathcal{L}$ Bethe roots in each set $\{x_{k,\ell}\}_{\ell=1}^{\mathcal{L}}$, they are allowed to be at $\pm\infty$, but at most one at each. The energy eigenvalue of $\mathcal{H}^{(k)}$ corresponding to the set of Bethe roots $\{x_{k,\ell}\}$ is given by

$$E^{(k)} \equiv E(\{x_{k,\ell}\}) = \mathrm{i}\left[\sum_{\ell=1}^{\mathcal{L}} \frac{1}{1 - \mathrm{i}\omega\, \mathrm{e}^{x_{k,\ell}}} - \frac{1}{6}\left(3 + \mathrm{i}\sqrt{3}\right)\mathcal{L}\right]. \tag{11}$$

Here we have used the property that sets of Bethe roots are invariant under complex conjugations, $\{x_{k,\ell}\}_{\ell=1}^{\mathcal{L}} \equiv \{x_{k,\ell}^*\}_{\ell=1}^{\mathcal{L}} \pmod{2\mathrm{i}\pi}$. Since the local Hamiltonians are Hermitian by construction, the energies (11) must be real. This reality of the energy imposes an additional physicality constraint on solutions to the Bethe equation (care must be taken to deal with roots at $\pm\infty$ appropriately). We note that all the root configurations considered below in the discussion of the spectrum of the system do satisfy this condition.

Let us remark that the Bethe equations (10) and the corresponding energies (11) of the $D(D_3)$ spin chain of even length $\mathcal{L}$ coincide with those of the three-state Potts spin chain with $\mathcal{L}/2$ sites [3]. We shall use this equivalence below to identify some of the thermodynamical properties of the $D(D_3)$ chain.

The energy eigenvalues of the *complete* Hamiltonian are characterized by two solutions to the Bethe equations (10). As a consequence of equations (6), (7) and along with (11) they are given by

$$E = \cos(\theta)\, E^{(1)} + \sin(\theta)\, E^{(2)} = \cos(\theta)\, E(\{x_{1,\ell}\}) + \sin(\theta)\, E(\{x_{2,\ell}\}), \tag{12}$$

provided these energies (or the corresponding root configurations) pair. Specifically, levels are said to pair if the two corresponding sets of Bethe roots form an eigenvalue of the transfer matrix, see equation (8). As the two sets of Bethe roots need not correspond to a unique eigenvalue of the transfer matrix, e.g. there may be two eigenvalues that differ by a constant factor or an eigenvalue might be degenerate, we refer to the total number of eigenvalues, including degeneracies, as the *pairing multiplicity*.

The total momentum of the corresponding state can also be given in terms of the two sets of Bethe roots: at $z_1 = 1 = z_2$ the transfer matrix becomes a shift operator by one site. Therefore the momentum operator is $P = -\mathrm{i} \ln t(1, 1)$. By construction the eigenvalues of this operator are real ($2\pi/\mathcal{L}$ times an integer for periodic boundary conditions considered here). Unlike for the energy (11) it is not possible to identify *partial* momentum contribution from one of the participating Bethe configurations uniquely [24]. Using the invariance of the sets of Bethe roots under complex conjugation we use

$$P^{(k)} \equiv P(\{x_{k,\ell}\}) = \mathrm{Re}\left[\frac{1}{\mathrm{i}} \sum_{\ell=1}^{\mathcal{L}} \ln(1 - \mathrm{i}\omega\, \mathrm{e}^{x_{k,\ell}})\right] = \frac{1}{2\mathrm{i}} \sum_{\ell=1}^{\mathcal{L}} \ln\left(\frac{1 - \mathrm{i}\omega\, \mathrm{e}^{x_\ell}}{1 - (1/\mathrm{i}\omega)\mathrm{e}^{x_\ell}}\right) \tag{13}$$

as definition of the partial momenta $P^{(k)}$. For later use we note that the second expression is *half* of the momentum of the three-state Potts spin chain [3]. Consistency with equation (8) implies that the *complete* momentum is related to the partial ones as

$$P = P^{(1)} - P^{(2)} + \mathrm{const.} \tag{14}$$

Again, roots $x_{k,\ell} = \pm\infty$ have to be taken into account to ensure finite (partial) momentum. The total momentum is given by the difference of partial momenta reflecting the fact $\mathcal{H}^{(2)}$ is the spatial inversion of $\mathcal{H}^{(1)}$. The remaining constant represents a macroscopic effect, details of which have been discussed in earlier works [24].

2.3.2. Braided chain. One closed chain proposed as an alternative to the periodic chain is the braided chain [25, 34, 38]. In this model, translational invariance is replaced by invariance under a global braiding operator. As a consequence the underlying symmetry of the model will not be broken, i.e. it has the full global $D(D_3)$ symmetry. The global Hamiltonians for these boundary conditions are defined by

$$\mathcal{H}^{(k)} = B h^{(k)}_{(\mathcal{L}-1)\mathcal{L}} B^{-1} + \sum_{j=1}^{\mathcal{L}-1} h^{(k)}_{j(j+1)}, \quad k \in \{1, 2\},$$

where

$$B = b_{12} b_{23} \ldots b_{(\mathcal{L}-1)\mathcal{L}}, \quad \text{and} \quad b = \lim_{z\to\infty}\left[\frac{1}{z^2} R(z, z)\right].$$

There also exist different possible definitions for the braiding operator b_i relating to other limits of $R(z_1, z_2)$ [21]. The integrability of the braided model is ensured by the existence of a transfer matrix $t(z_1, z_2)$, which can be found in [21]. Eigenstates of this model are again characterized

by the Bethe equations (10). As in the periodic case there must be $\mathcal{L}$ Bethe roots, this time with one Bethe root allowed at $+\infty$ but none allowed at $-\infty$.

As mentioned above, the Hamiltonian of this model is invariant under the action of the global braiding operator. Specifically, we find that B can be realized by the transfer matrix of the braided model as $B = t(1, 1)$. Furthermore, the braiding operator is idempotent: from the analysis of small systems we find that

$$B^n = I \quad \text{when} \quad \begin{cases} n = 3\mathcal{L}, & \mathcal{L} \text{ even}, \\ n = 2\mathcal{L}, & \mathcal{L} \text{ odd}. \end{cases} \tag{15}$$

This allows us to define an analogue of the momentum operator as the generator of braiding operations by $P_\mathrm{b} = -\mathrm{i} \ln B$. The eigenvalues of P_b are restricted to integer multiples of either $\frac{\pi}{\mathcal{L}}$ or $\frac{2\pi}{3\mathcal{L}}$ depending on the parity of $\mathcal{L}$.

2.3.3. Open boundary conditions. We also consider spin chains with open boundary conditions. In this case integrable models are derived from representations of Sklyanin's reflection algebra [57]. c-number representations of this algebra define possible boundary terms. For the present model, these K-matrices are found to be the same as have been determined for the $D(D_3)$ one-parameter R-matrix [13]. The global Hamiltonians are

$$\mathcal{H}^{(k)} = \chi_k^- B_1^{(k)-} + \chi_k^+ B_\mathcal{L}^{(k)+} + \sum_{j=1}^{\mathcal{L}-1} h_{j(j+1)}^{(k)}.$$

Here, the boundary operators $B^{(k)-}$ ($B^{(k)+}$) act on the first (last) site of the chain, respectively. There exist three possible (independent) options for each of these operators, namely

$$B^{(1)-}, (B^{(1)+})^*, (B^{(2)-})^*, B^{(2)+} \in \left\{ \begin{pmatrix} 0 & \omega^2 b & \omega^2 b^2 \\ \omega b^2 & 0 & b \\ \omega b & b^2 & 0 \end{pmatrix} \middle| \, b = 1, \omega, \omega^2 \right\}. \tag{16}$$

The real boundary amplitudes where $\chi_k^\pm$, $k \in \{1, 2\}$, have to satisfy $\chi_1^+ \chi_2^+ = \chi_1^- \chi_2^- = 0$. Like the periodic and braided models integrability is derived from the existence of a transfer matrix (see [21, 24] for the open $D(D_3)$ transfer matrix) and the eigenstates of the Hamiltonian are classified by sets of Bethe roots. The Bethe equations for the Hamiltonian $\mathcal{H}^{(k)}$ are independent of the choice of the boundary operators, $B^{(k)\pm}$,

$$\prod_{l=1}^{d_k} \left(\frac{\mathrm{e}^{x_{k,l}} - \omega^2 \mathrm{e}^{x_{k,j}}}{\mathrm{e}^{x_{k,l}} - \omega \mathrm{e}^{x_{k,j}}} \right) = (-1)^{\mathcal{L}+1} \left(\frac{1 + \omega \mathrm{e}^{2x_{k,j}}}{1 + \omega^2 \mathrm{e}^{2x_{k,j}}} \right) \left(\frac{1 - \omega^2 \mathrm{e}^{2x_{k,j}}}{1 - \omega \mathrm{e}^{2x_{k,j}}} \right) \left(\frac{1 + \mathrm{i}\omega^2 \mathrm{e}^{x_{k,j}}}{1 - \mathrm{i}\omega \mathrm{e}^{x_{k,j}}} \right)^{2\mathcal{L}}$$
$$\times \Phi(x_{k,j}, \chi_k^-) \Phi(x_{k,j}, \chi_k^+) \tag{17}$$

with Bethe roots always appearing in pairs of $\pm x$ and where

$$\Phi(x, \chi) = \begin{cases} 1 & \text{for } \chi = 0, \\ \left(\dfrac{\chi\sqrt{3}(1 - \omega \mathrm{e}^{2x}) + \mathrm{i}\omega^2 \left(1 + \chi\sqrt{3}\right) \mathrm{e}^x}{\chi\sqrt{3}(1 - \omega^2 \mathrm{e}^{2x}) - \mathrm{i}\omega \left(1 + \chi\sqrt{3}\right) \mathrm{e}^x} \right) & \text{for } \chi \neq 0. \end{cases}$$

In addition to the explicit dependence of the Bethe equations on the boundary amplitudes $\chi_k^\pm$ the latter determine the number d_k of Bethe roots $x_{k,j}$: for the open chain with free ends, i.e. $\chi_k^\pm = 0$,

there are $d_k = 2\mathcal{L}$ Bethe roots with at most one pair of roots at $\pm\infty$ [24]. A non-zero boundary term at one end of the chain, i.e. choosing one of either χ_k^+ or χ_k^- non-zero, changes the number of roots to $d_k = 2\mathcal{L}+2$, while for boundary terms at both ends there are $d_k = 2\mathcal{L}+4$ Bethe roots. We refer to the extra pairs of roots appearing as compared to the free-ends case as boundary roots[2].

These boundary roots are finite for non-zero boundary amplitudes $\chi_k^\pm$ but approach $\pm\infty$ in the limit of free ends.

The energy of the open boundary Hamiltonian $\mathcal{H}^{(k)}$ corresponding to a solution of equations (17) is given by

$$E^{(k)}(\{x_{k,\ell}\}) = \frac{\mathrm{i}}{2}\left\{\sum_{l=1}^{d_k}\left[\frac{1}{1-\mathrm{i}\omega\,\mathrm{e}^{x_{k,l}}}\right] - \left(1-\mathrm{i}\frac{\sqrt{3}}{3}\right)\mathcal{L} - \phi(\chi_k^+) - \phi(\chi_k^-)\right\},$$

where

$$\phi(\chi) = \begin{cases} 0 & \text{for } \chi = 0, \\ 1+\mathrm{i}\chi & \text{for } \chi \neq 0. \end{cases}$$

Again we note that the energy eigenvalues are real as the global Hamiltonian is Hermitian. Additionally, it is important to note that the presence of boundary interactions breaks the $D(D_3)$ invariance of the model. Only for free ends the open model has this invariance.

2.4. Fusion path analogues

As the local Hamiltonians have the symmetry of $D(D_3)$ it is possible to create fusion path analogues [22]. Depending on the boundary conditions imposed the global Hamiltonians may or may not be equivalent to their spin formalism counterparts discussed above. The construction of the analogous fusion path chains uses the Pasquier's method of representation theory reliant face-vertex correspondence [54]. This allows the fusion path analogues to be considered as the Hamiltonian limits of RSOS models and proves their integrability. The connection between fusion IRF models and many other physical systems has already been established [28].

We first define the fusion path basis. Basis vectors of the fusion path space are of the form

$$|a_0 a_1 \ldots a_{\mathcal{L}}\rangle\,,$$

where $a_i \in \{\mathfrak{a}, \mathfrak{b}, \mathfrak{c}, \mathfrak{d}, \mathfrak{e}, \mathfrak{f}, \mathfrak{g}, \mathfrak{h}\}$ and neighbouring labels satisfy the condition

$$a_i a_{i+1} \in \{ab \mid V_b \subset V_a \otimes V_{\mathfrak{g}}\}$$
$$= \{\mathfrak{ag}, \mathfrak{bh}, \mathfrak{cg}, \mathfrak{ch}, \mathfrak{dg}, \mathfrak{dh}, \mathfrak{eg}, \mathfrak{eh}, \mathfrak{fg}, \mathfrak{fh}, \mathfrak{ga}, \mathfrak{gc}, \mathfrak{gd}, \mathfrak{ge}, \mathfrak{gf}, \mathfrak{hb}, \mathfrak{hc}, \mathfrak{hd}, \mathfrak{he}, \mathfrak{hf}\}. \tag{18}$$

Thus a_{i+1} must appear in the fusion of a_i and $\mathfrak{g}$. Diagrammatically, a basis vector corresponds to the figure below, where the joining of two lines indicates fusion which occurs from left to right and top to bottom;

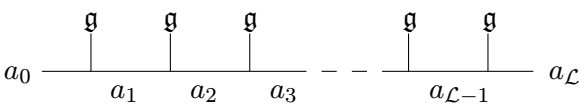

[2] It is important to note that for $\chi_k^\pm$ small the presences of the boundary Bethe roots will not have a significant effect on the configuration of the bulk Bethe roots.

To construct local operators on this space we utilize F-moves (generalized 6–j symbols), which allow the temporary recording of fusion,

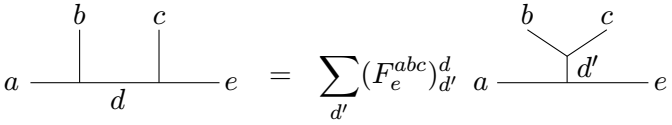

$$= \sum_{d'} (F_e^{abc})_{d'}^{d}$$

In terms of these F-moves, we can define two-site projection operators which act non-trivially on a single link i of the fusion path lattice[3],

$$\tilde{p}^{(b)}_{i-1,i,i+1} = \sum_{a_{i-1},a_i,a_i',a_{i+1}} \left[\left(F^{a_{i-1}\mathfrak{g}\mathfrak{g}}_{a_{i+1}} \right)^{a_i'}_{b} \right]^* \left(F^{a_{i-1}\mathfrak{g}\mathfrak{g}}_{a_{i+1}} \right)^{a_i}_{b} \left| ..a_{i-1}a_i'a_{i+1}.. \right\rangle \left\langle ..a_{i-1}a_ia_{i+1}.. \right| .$$

The unitary F-moves associated with $D(D_3)$ can be calculated explicitly from the representation theory of $D(D_3)$ [56]. Below we shall consider local interactions defined analogously to the nearest-neighbour spin chain ones, equation (5):

$$\tilde{h}^{(1)} = \frac{2\sqrt{3}}{3}\tilde{p}^{(\mathfrak{a})} - \frac{\sqrt{3}}{3}\tilde{p}^{(\mathfrak{c})} - \frac{\sqrt{3}}{3}\tilde{p}^{(\mathfrak{d})} - \frac{\sqrt{3}}{3}\tilde{p}^{(\mathfrak{e})} + \frac{2\sqrt{3}}{3}\tilde{p}^{(\mathfrak{f})},$$

$$\tilde{h}^{(2)} = \frac{2\sqrt{3}}{3}\tilde{p}^{(\mathfrak{a})} - \frac{\sqrt{3}}{3}\tilde{p}^{(\mathfrak{c})} - \frac{\sqrt{3}}{3}\tilde{p}^{(\mathfrak{d})} + \frac{2\sqrt{3}}{3}\tilde{p}^{(\mathfrak{e})} - \frac{\sqrt{3}}{3}\tilde{p}^{(\mathfrak{f})}.$$

Note that these Hamiltonians act on three consecutive labels of the fusion path basis but only can change the middle label.

As a consequence of the equivalence of the local interactions between the spin and fusion path formalisms, the global models in the two formalisms may differ only by boundary conditions. The open model with free ends and braided model both have $D(D_3)$ invariance which means that the fusion path and spin versions of these chains are equivalent. This implies that the energy spectra are identical and the degeneracies appearing in each formalism are related via a mapping. For convenience we use the degeneracy of the spin chain formalism for these choices of boundary conditions. For periodic boundary conditions, however, neither the spin chain nor fusion path model has the complete $D(D_3)$ invariance and thus the two models, while sharing bulk properties, are distinct [22].

To construct a periodic model in the fusion path basis, we need to consider the space spanned by the basis vectors satisfying $a_0 = a_{\mathcal{L}}$. As a consequence of the fusion rules, this periodic closure is possible only for lattices of even length $\mathcal{L}$. Furthermore, they lead to the decomposition of the Hilbert space

$$\text{Hilbert space} = \mathbb{C}\left\{ |a_1 \ldots a_{\mathcal{L}}\rangle \; | a_1 = \mathfrak{g} \text{ or } a_1 = \mathfrak{h} \right\} \oplus \mathbb{C}\left\{ |a_1 \ldots a_{\mathcal{L}}\rangle \; | a_2 = \mathfrak{g} \text{ or } a_2 = \mathfrak{h} \right\}, \tag{19}$$

where each of these subspaces has dimension $3^{\mathcal{L}} + 1$. The global Hamiltonians are

$$\tilde{\mathcal{H}}^{(k)} = \tilde{h}^{(k)}_{(\mathcal{L}-1)\mathcal{L}1} + \tilde{h}^{(k)}_{\mathcal{L}12} + \sum_{j=2}^{\mathcal{L}-1} \tilde{h}^{(k)}_{(j-1)j(j+1)}, \quad k \in \{1, 2\}.$$

The integrability of this model can be established based on the existence of an R-matrix connected to an RSOS model whose heights correspond to the labels of the irreps of $D(D_3)$.

[3] It is important for the reader to note that in this fusion path formalism the labels in the basis vectors do not correspond to individual sites but rather bonds. The individual sites are still the $\mathfrak{g}$-anyons but now cannot be solely acted on as this would break local $D(D_3)$ invariance.

As the R-matrix of equation (4) is expressible in terms of the $D(D_3)$ projection operators, it follows that there exists an equivalent operator in the fusion path basis [54],

$$\begin{aligned}\tilde{R}(z_1, z_2) &= f_{\mathfrak{a}}(z_1, z_2)\tilde{p}^{(\mathfrak{a})} + f_{\mathfrak{c}}(z_1, z_2)\tilde{p}^{(\mathfrak{c})} + f_{\mathfrak{d}}(z_1, z_2)\tilde{p}^{(\mathfrak{d})} + f_{\mathfrak{e}}(z_1, z_2)\tilde{p}^{(\mathfrak{e})} + f_{\mathfrak{f}}(z_1, z_2)\tilde{p}^{(\mathfrak{f})} \\ &= \sum_{a_1, a_2, a_2', a_3} B\begin{pmatrix} a_1 & a_2' \\ a_2 & a_3 \end{pmatrix} z_1, z_2 \Big) \left|a_1 a_2' a_3\right\rangle \left\langle a_1 a_2 a_3\right|, \end{aligned} \tag{20}$$

satisfying a face Yang–Baxter equation

$$\tilde{R}_{123}(x_1, x_2)\tilde{R}_{234}(x_1 y_1, x_2 y_2)\tilde{R}_{123}(y_1, y_2) = \tilde{R}_{234}(y_1, y_2)\tilde{R}_{123}(x_1 y_1, x_2 y_2)\tilde{R}_{234}(x_1, x_2).$$

The weights appearing in $\tilde{R}(z_1, z_2)$ are used to construct the commuting transfer matrix [32]

$$\left\langle a_1' \ldots a_{\mathcal{L}}'\right| \tilde{t}(z_1, z_2) \left|a_1 \ldots a_{\mathcal{L}}\right\rangle = \prod_{j=1}^{\mathcal{L}} B\begin{pmatrix} a_j' & a_{j+1}' \\ a_j & a_{j+1} \end{pmatrix} z_1, z_2 \Big).$$

Once again this transfer matrix generates a family of commuting operators, including the global Hamiltonians $\tilde{\mathcal{H}}^{(1)}$ and $\tilde{\mathcal{H}}^{(2)}$, implying integrability. Again, the dependence of the transfer matrix on two spectral parameters guarantees commutativity of the two components

$$\left[\tilde{\mathcal{H}}^{(1)}, \tilde{\mathcal{H}}^{(2)}\right] = 0.$$

Through the analysis of small finite-size systems we are able to make two important observations. Firstly, we find that the eigenvalues $\tilde{\Lambda}(z_1, z_2)$ of the fusion path transfer matrix factorize into two polynomials of degree $\mathcal{L}$ in the same manner as those in the spin chain case (8). Secondly, we find that the eigenvalues satisfy functional relations similar to equations (9), i.e.

$$\begin{aligned}&\lambda_1(z_1)\tilde{\Lambda}(z_1, z_2) = (\omega z_1 + 1)^{\mathcal{L}}\tilde{\Lambda}(\omega z_1, z_2) \pm (z_1 - 1)^{\mathcal{L}}\tilde{\Lambda}(\omega^{-1} z_1, z_2), \\ &\lambda_2(z_2)\left[\tilde{\Lambda}(z_1, z_2)\right]^* = (\omega z_2 + 1)^{\mathcal{L}}\left[\tilde{\Lambda}(z_1, \omega z_2)\right]^* \pm (z_2 - 1)^{\mathcal{L}}\left[\tilde{\Lambda}(z_1, \omega^{-1} z_2))\right]^*. \end{aligned} \tag{21}$$

Again, $\lambda_k(z)$ are analytic functions. The $\pm$ sign depends upon the eigenvalue in question. Preliminary calculations indicate that this relation can be obtained using the fusion procedure for RSOS models [7, 43]. Like the periodic spin chain case these functional relations lead to Bethe equations which have to be satisfied by the zeros of the transfer matrix eigenvalues

$$(-1)^{\mathcal{L}+1}\left(\frac{1 + (\mathrm{i}/\omega)\,\mathrm{e}^{x_{k,j}}}{1 - \mathrm{i}\omega\,\mathrm{e}^{x_{k,j}}}\right)^{\mathcal{L}} = \eta\prod_{l=1}^{\mathcal{L}}\frac{\mathrm{e}^{x_{k,l}} - (1/\omega)\,\mathrm{e}^{x_{k,j}}}{\mathrm{e}^{x_{k,l}} - \omega\,\mathrm{e}^{x_{k,j}}}, \quad j = 1, \ldots, \mathcal{L}, \tag{22}$$

where $\eta = \pm 1$ corresponds to the allowed signs in the functional relations (21). This sign was not present in the Bethe equations for the spin chain (10) indicating the likely presence of different excitations. As before, every set of roots $\{x_{k,\ell}\}$ solving the Bethe equations (22) parametrizes an eigenvalue of the fusion path model. The energy eigenvalue of $\tilde{\mathcal{H}}^{(k)}$ is again given by equation (11).

In previous studies of anyonic fusion path models [20, 37], integrability was also observed by relating them to transfer matrices associated with RSOS models. However, in these instances the fusion path R-matrices corresponded to representations of the Temperley–Lieb algebra. Every RSOS model can be naturally associated with a graph where nodes represent the labels of anyons in the theory which are connected if they can appear next to each other in the fusion path basis as given by equation (18), see [53]. For the $D(D_3)$ model considered here

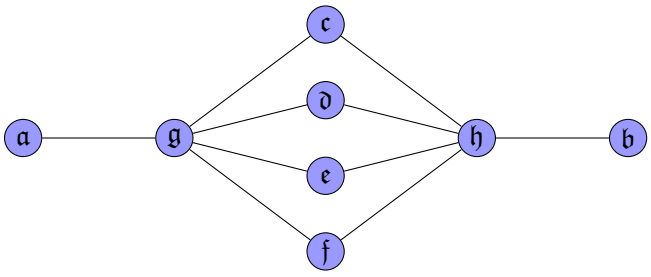

Figure 1. A graphical representation of allowed neighbouring labels in the fusion path chain. The vertices/nodes of the graphs are the labels of anyons which are connected via an edge if and only if the two anyon labels can appear next to each as given by equation (18).

we obtain the graph given in figure 1. This graph is equivalent to McKay's representation graph for the representation $\pi_{\mathfrak{g}}$ of $D(D_3)$ [48]. We note that this graph shows that the $D(D_3)$ fusion path model does not correspond to any of the known RSOS models associated with Dynkin diagrams [52, 53, 55, 62]. It also does not appear among the more general graphs associated with other RSOS models [16].

3. The Bethe equations and exact results for spin chains

As a consequence of equation (12) the ground state energy of the model is always obtained by the following combinations (NB: provided that these states are allowed to pair) [24]:

$$E_0 = \begin{cases} \cos(\theta)E_{\mathrm{l}}^{(1)} + \sin(\theta)E_{\mathrm{l}}^{(2)}, & 0 \leqslant \theta < \frac{\pi}{2}, \\ \cos(\theta)E_{\mathrm{h}}^{(1)} + \sin(\theta)E_{\mathrm{l}}^{(2)}, & \frac{\pi}{2} \leqslant \theta < \pi, \\ \cos(\theta)E_{\mathrm{h}}^{(1)} + \sin(\theta)E_{\mathrm{h}}^{(2)}, & \pi \leqslant \theta < \frac{3\pi}{2}, \\ \cos(\theta)E_{\mathrm{l}}^{(1)} + \sin(\theta)E_{\mathrm{h}}^{(2)}, & \frac{3\pi}{2} \leqslant \theta < 2\pi. \end{cases} \tag{23}$$

Here $E_{\mathrm{l}}^{(k)}$ is the lowest energy of the $\mathcal{H}^{(k)}$ and $E_{\mathrm{h}}^{(k)}$ is the highest. An immediate implication of this form of the ground state energy is that there are level crossings for θ being integer multiples of $\frac{\pi}{2}$ leading to first-order quantum phase transitions. Here we will use a different consequence of (23): the complete spectrum of the model can be obtained from an analysis at these particular points in combination with the implementation of the pairing rules [24]. An additional simplification arises from the fact that the spectra of $\mathcal{H}^{(1)}$ and $\mathcal{H}^{(2)}$ are identical for most boundary conditions considered in this paper: this allows us to restrict the analysis of the low-energy spectrum to those of the Hamiltonians $\mathcal{H}_{\theta=0} = \mathcal{H}^{(1)}$ and $\mathcal{H}_{\theta=\pi} = -\mathcal{H}^{(1)}$ whose ground state energies are $E_{\mathrm{l}}^{(1)} = E_{\mathrm{l}}^{(2)}$ and $-E_{\mathrm{h}}^{(1)} = -E_{\mathrm{h}}^{(2)}$, respectively. Only in the case of open boundary conditions with $D(D_3)$-symmetry breaking boundary fields, the spectra of $\pm\mathcal{H}^{(1)}$ and $\pm\mathcal{H}^{(2)}$ are independent.

3.1. Energy density in the thermodynamical limit

The study of the excitation spectrum of a model requires knowledge of the bulk properties. As such we recall previously obtained results and present them here for completeness [24].

In the thermodynamic limit $\mathcal{L} \to \infty$ bulk properties of the system are independent of the boundary conditions imposed. Therefore, we can compute the energy density from the Bethe equations (10) for the periodic spin chain. To this end the solutions to the Bethe equations need to be classified and the root configurations corresponding to the ground state and low-energy excitations have to the identified. As mentioned above, the Bethe equations for the periodic $D(D_3)$ spin chain arise also in the context of the three-state Potts model. For the latter, the classification of solutions has been obtained by Albertini *et al* [2, 3], see also [24]. In particular, numerical diagonalization of the transfer matrix shows that the lowest energy states of $\mathcal{H}_{\theta=\pi}$ consist of three different Bethe root ($z_l \equiv z_{1,l}$) types:

1. positive Bethe roots (+-string), $z_l = \mathrm{i}\omega\, \mathrm{e}^{x_l^+}$, where $x_l^+ \in \mathbb{R}$,
2. negative Bethe roots (−-string), $z_l = \mathrm{i}\omega\, \mathrm{e}^{x_l^- + \mathrm{i}\pi}$, where $x_l^- \in \mathbb{R}$,
3. two-strings, where the Bethe roots come in pairs, $z_l = \mathrm{i}\omega\, \mathrm{e}^{x_l^s + \frac{2\mathrm{i}\pi}{3}}$, $z_{l+1} = \mathrm{i}\omega\, \mathrm{e}^{x_l^s - \frac{2\mathrm{i}\pi}{3}}$ with $x_l^s \in \mathbb{R}$,

as well as a limited number of Bethe roots at $\pm\infty$. Letting N_+, N_- and N_2 be the number of +-strings, −-strings and two-strings, respectively, and setting $n_{\pm\infty} \in \{0, 1\}$ to be the number of Bethe roots at $\pm\infty$ then we have the constraint

$$N_+ + N_- + 2N_s = \mathcal{L} - n_{+\infty} - n_{-\infty}.$$

In the three-states Potts model these root types were also identified, along with a few other which we do not consider, with the additional constraint $n_{+\infty} = n_{-\infty}$ [3].

Allowing combinations of these roots we then find that the for the periodic Hamiltonian we can take the logarithm of the Bethe equations and define the following set of counting functions:

$$Z_+(x) = -\phi\left(x; \frac{7}{12}\right) + \frac{1}{\mathcal{L}}\sum_{l=1}^{N_+}\phi\left(x - x_l^+; \frac{1}{3}\right) + \frac{1}{\mathcal{L}}\sum_{l=1}^{N_-}\phi\left(x - x_l^-; \frac{5}{6}\right) + \frac{1}{\mathcal{L}}\sum_{l=1}^{N_s}\phi\left(x - x_l^s; \frac{2}{3}\right),$$

$$Z_-(x) = -\phi\left(x; \frac{1}{12}\right) + \frac{1}{\mathcal{L}}\sum_{l=1}^{N_+}\phi\left(x - x_l^+; \frac{5}{6}\right) + \frac{1}{\mathcal{L}}\sum_{l=1}^{N_-}\phi\left(x - x_l^-; \frac{1}{3}\right) + \frac{1}{\mathcal{L}}\sum_{l=1}^{N_s}\phi\left(x - x_l^s; \frac{1}{6}\right),$$

$$Z_s(x) = \left[\phi\left(x; \frac{11}{12}\right) + \phi\left(x; \frac{1}{4}\right)\right] - \frac{1}{\mathcal{L}}\sum_{k=1}^{N_+}\phi\left(x - x_l^+; \frac{2}{3}\right) - \frac{1}{\mathcal{L}}\sum_{l=1}^{N_-}\phi\left(x - x_l^-; \frac{1}{6}\right) - \frac{1}{\mathcal{L}}\sum_{l=1}^{N_s}\phi\left(x - x_l^s; \frac{1}{3}\right),$$

where

$$\phi(x; t) = -\frac{1}{\pi}\tan^{-1}\left(\frac{\tanh(\frac{x}{2})}{\tan(t\pi)}\right).$$

In the thermodynamical limit, we find that the ground state for $\mathcal{H}_{\theta=\pi}$ consists entirely of two-strings [3, 24]. For finite-size systems this configuration is only realized when $\mathcal{L}$ is even. The lowest energy Bethe root configuration for odd $\mathcal{L}$ is given by $\frac{\mathcal{L}-1}{2}$ two-strings and one $\pm$-string.

Similarly, we find that the lowest energy states of $\mathcal{H}_{\theta=0}$ consist of the same three Bethe root types and hence we have the same counting functions. In the thermodynamical limit the Bethe root configuration of the ground state consists of only negative and positive Bethe roots appearing in the ratio of three −-strings to one +-string. For finite-size systems this configuration

is only realized when $\mathcal{L}$ is a multiple of four. The lowest energy Bethe root configuration for the other chain lengths also consists of only negative and positive Bethe roots appearing approximately in the ratio 3:1.

Based on these observations the root density formalism [63] can be applied to compute the corresponding energy densities: the density of two-strings in the thermodynamic ground state of $\mathcal{H}_{\theta=\pi}$ and their dressed energies $\mathcal{H}_{\theta=\pi}$ are determined by linear integral equations

$$\begin{aligned}\rho(x) &= \frac{1}{\pi}\left(\frac{1}{4\cosh(x)-2\sqrt{3}} - \frac{1}{2\cosh(x)}\right) + \frac{\sqrt{3}}{2\pi}\int_{-\infty}^{\infty} \mathrm{d}y\, \frac{1}{2\cosh(x-y)+1}\rho(y),\\ \epsilon(x) &= \frac{1}{4\cosh(x)-2\sqrt{3}} - \frac{1}{2\cosh(x)} + \frac{\sqrt{3}}{2\pi}\int_{-\infty}^{\infty} \mathrm{d}y\, \frac{1}{2\cosh(x-y)+1}\epsilon(y).\end{aligned} \tag{24}$$

These equations (and the corresponding ones for $\mathcal{H}_{\theta=0}$) can be solved by Fourier transformation giving the ground state energy densities [3, 24, 35]

$$\frac{1}{\mathcal{L}}E_{\theta=\pi} = -\left[\frac{1}{\pi}+\frac{2\sqrt{3}}{9}\right] \quad \text{and} \quad \frac{1}{\mathcal{L}}E_{\theta=0} = -\left[\frac{1}{2\pi}-\frac{2\sqrt{3}}{9}+\frac{3}{4}\right]. \tag{25}$$

3.2. Fermi velocity

The low-energy excitations over these ground states have a linear dispersion and their Fermi velocities have been computed within the root density formalism in the context of the three-state Potts model [3]. As discussed above, it is possible to identify energy and momentum eigenvalues of this model with those of the partial Hamiltonians $\mathcal{H}^{(k)}$ (11) and corresponding momenta (13) using the equivalence of the corresponding Bethe equations.

Noting that the contribution of a single two-string to the partial momentum can be expressed in terms of their density in the thermodynamic limit

$$p(x) = \pi\int^{x} \mathrm{d}y\, \rho(y), \tag{26}$$

we can eliminate the rapidity x from equations (24) and (26) to obtain the dispersion relation $\epsilon(p)$ of two-strings. Therefore, the Fermi velocity of low-lying excitations of $\mathcal{H}_{\theta=\pi}$ is found to be

$$v_{\mathrm{F}} = \left.\frac{\partial\epsilon(p)}{\partial p}\right|_{p=p_{\mathrm{F}}} = \left.\frac{1}{\pi}\frac{\epsilon'(x)}{\rho(x)}\right|_{x=-\infty} = 3 \tag{27}$$

in agreement with the finite-size analysis of the spectrum performed in [23].

Similarly we can compute the Fermi velocity of gapless excitations for the Hamiltonian $\mathcal{H}_{\theta=0}$. Again the result is twice than what has been found for the three-state Potts chain [3], i.e. $v_{\mathrm{F}} = \frac{3}{2}$.

3.3. Boundary fields

We can also determine the exact expressions for the surface energy, i.e. the $\mathcal{L}^0$ contributions to the energy, for the open model with interacting boundary fields. Firstly, we find the ground energy for the Hamiltonians $\mathcal{H}_{\theta=\pi}$ and $\mathcal{H}_{\theta=0}$, and then extend this result to generic θ using equation (23). Starting with the Bethe equations (17) we can apply the same method that was used to calculate bulk energy density in section 3.1. For the open spin chain with free ends the

surface energy has been computed previously [24]. Due to the symmetry of the Bethe equations the general case can be studied in the context of the open chain with a single boundary field present, e.g. $\chi_1^+ \neq 0$ and all other boundary amplitudes vanishing, and compute the correction to case of the free ends.

For even $\mathcal{L}$ and χ_1^+ not too large the Bethe root configuration corresponding to the ground state of $\mathcal{H}_{\theta=\pi}$ consists of $\mathcal{L}$ two-strings, distributed symmetrically around the imaginary axis (just as in the free-ends case [24]) and, in addition two boundary Bethe roots. The latter are found to be either $\pm$-strings depending on the sign of χ_1^+. As the magnitude of χ_1^+ is decreased these boundary Bethe roots tend towards $\pm\infty$ to recover the Bethe configurations of the free-ends model[4]. We find that the correction to surface energy for the Hamiltonian $\mathcal{H}_{\theta=\pi}$ with one interacting boundary field, compared to the free ends case, is

$$g_{\theta=\pi}(\chi) = -\frac{2\chi^2\sqrt{3}}{1+2\chi\sqrt{3}} - \frac{18\chi^3\sqrt{3}}{\pi(1+2\chi\sqrt{3})\sqrt{1+2\chi\sqrt{3}-9\chi^2}} \begin{cases} \operatorname{arccosh}\left(-\frac{1}{2}-\frac{1}{2\chi\sqrt{3}}\right), & \chi<0, \\ 0, & \chi=0, \\ \operatorname{arccosh}\left(\frac{1}{2}+\frac{1}{2\chi\sqrt{3}}\right), & \chi>0. \end{cases}$$

Similarly, we find the surface energy correction for $\mathcal{H}_{\theta=0}$,

$$g_{\theta=0}(\chi) = \frac{2\chi^2\sqrt{3}}{1+2\chi\sqrt{3}} - \begin{cases} \dfrac{-9\chi\sqrt{-\chi}}{2(1+2\chi\sqrt{3})\sqrt{\sqrt{3}-3\chi}} + \dfrac{9\chi^3\sqrt{3}\operatorname{arccosh}\left(-\frac{1}{2}-\frac{1}{2\chi\sqrt{3}}\right)}{\pi(1+2\chi\sqrt{3})\sqrt{1+2\chi\sqrt{3}-9\chi^2}}, & \chi<0, \\ 0, & \chi=0, \\ \dfrac{9\chi\sqrt{\chi}}{2\sqrt{\sqrt{3}+9\chi}} + \dfrac{9\chi^3\sqrt{3}\operatorname{arccosh}\left(\frac{1}{2}+\frac{1}{2\chi\sqrt{3}}\right)}{\pi(1+2\chi\sqrt{3})\sqrt{1+2\chi\sqrt{3}-9\chi^2}}, & \chi>0. \end{cases}$$

Formally, the calculation of these corrections requires $-\frac{1}{3\sqrt{3}} < \chi < \frac{1}{\sqrt{3}}$. The restriction to this interval is due to the change in the analytical behaviour of the Bethe equations which is reflected by the presence of poles in the above expressions.

Putting these results together we are able to determine the ground state energies of $\mathcal{H}_{\theta=\pi}$ and $\mathcal{H}_{\theta=0}$ up to order $\mathcal{L}^0$

$$E_{\theta=\pi}(\chi_1^+, \chi_1^-) = -\left[\frac{1}{\pi}+\frac{2\sqrt{3}}{9}\right]\mathcal{L} + \left[\frac{3}{2}-\frac{2\sqrt{3}}{3}\right] + g_{\theta=\pi}(\chi_1^+) + g_{\theta=\pi}(\chi_1^-) + o(\mathcal{L}^0),$$

$$E_{\theta=0}(\chi_1^+, \chi_1^-) = -\left[\frac{1}{2\pi}-\frac{2\sqrt{3}}{9}+\frac{3}{4}\right]\mathcal{L} + \left[-\frac{3}{4}+\frac{2\sqrt{3}}{3}\right] + g_{\theta=0}(\chi_1^+) + g_{\theta=0}(\chi_1^-) + o(\mathcal{L}^0). \quad (28)$$

In figure 2 we plot the predicted functions $g_{\theta=\pi}(\chi)$ and $g_{\theta=0}(\chi)$ compared to the equivalent numerical values obtained by solving the Bethe equations (with $\chi_1^- = \chi_2^\pm = 0$).

Although the numerical values have been obtained for only 100 sites, we clearly see that values match the analytically predicted results, both inside and outside the region $-\frac{1}{3\sqrt{3}} < \chi < \frac{1}{\sqrt{3}}$. The numerical solution of the Bethe equations for larger boundary amplitudes is limited by numerical instabilities resulting from, e.g. boundary Bethe roots passing the other Bethe roots.

[4] On a technical note, it was observed that the magnitude of the boundary Bethe roots will also increase as $\mathcal{L}$ increases for fixed χ. We assume that as $\mathcal{L}$ goes to ∞ the boundary Bethe roots tend to $\pm\infty$ for fixed boundary amplitudes $\chi_k^\pm$. This is important when considering the thermodynamical limit.

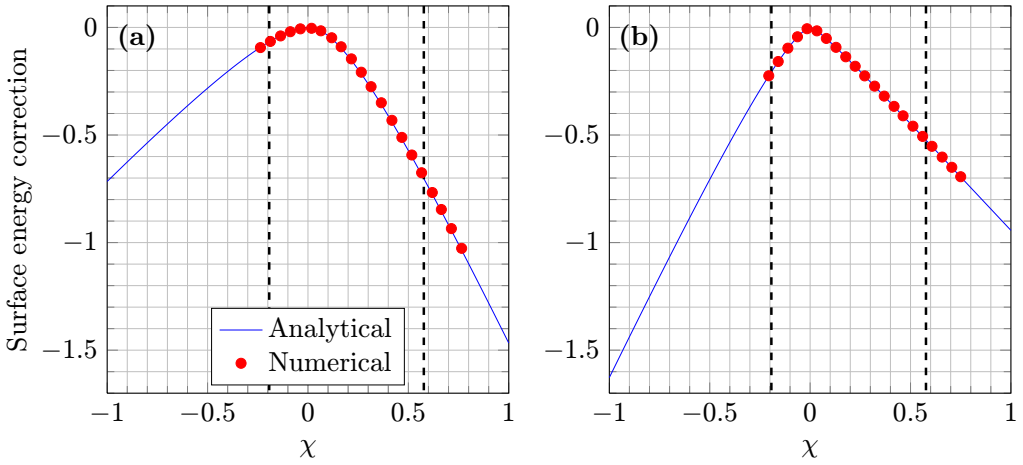

Figure 2. Numerical values of the correction to the surface energies for the Hamiltonians (a) $\mathcal{H}_{\theta=\pi}$ and (b) $\mathcal{H}_{\theta=0}$ as a function of the boundary amplitude χ obtained solving the Bethe equations for a system of 100 sites compared to the analytical predictions $g_{\theta=\pi}(\chi)$ and $g_{\theta=0}(\chi)$, respectively. Dashed lines indicate the range, $-\frac{1}{3\sqrt{3}} < \chi < \frac{1}{\sqrt{3}}$, where the former expressions were formally derived.

The asymptotic behaviour of the surface energy corrections for large χ does, however, coincide with what is expected from the corresponding eigenvalues of the boundary operators $B^{(k)\pm}$ (16), i.e. -1 and 2. This leads us to conjecture that the energies are analytically correct for all values of $\chi_k^{\pm} \in \mathbb{R}$.

Using equation (23) along with the relations,

$$E_{\mathrm{h}}^{(k)} = -E_{\theta=\pi}(\chi_k^+, \chi_k^-) \quad \text{and} \quad E_1^{(k)} = E_{\theta=0}(\chi_k^+, \chi_k^-),$$

we are able to determine the ground state energy of $\mathcal{H}_\theta$ for generic θ. We should again recall that we have the constraint $\chi_1^+\chi_2^+ = \chi_1^-\chi_2^- = 0$ and that the interacting boundary terms break the $D(D_3)$ invariance of the model.

4. Excitations and conformal field theories

The presence of a coupling parameter makes the identification of a CFT a difficult task. Every energy level of the Hamiltonian depends on the coupling parameter θ, moreover which of the energies is the lowest will change with θ. This implies that the model cannot be described by a single CFT but rather but multiple ones. To simplify the issue we first study the model at the level crossings, i.e. for coupling parameters being integer multiples of $\frac{\pi}{2}$. As discussed above the energy spectrum at these points is that of the partial Hamiltonians $\mathcal{H}_{\theta=0} = \mathcal{H}^{(1)}$ and $\mathcal{H}_{\theta=\pi} = -\mathcal{H}^{(1)}$ (up to degeneracies). For these we can use powerful machinery to accurately describe the model at these special points. It turns out that the low-energy effective theories of the partial models are given by minimal models.

Once the critical theories at these special couplings have been identified it is a relatively straightforward, albeit non-trivial, task to obtain the conformal operator content of the complete model for general coupling θ: the main difficulties come with identifying the previously mentioned pairing rules and connecting them with some conserved quantity of the model.

To make the presentation self-contained we begin by presenting our results on the low-energy spectrum of the periodic spin chain reported previously [23, 24] with an extended discussion of the residual $D(D_3)$ symmetry under these boundary conditions and the pairing rules. This section is followed by new results of our studies of the critical properties of the periodic fusion path chain and the models with braided and open boundary conditions.

4.1. Periodic spin chain

As discussed above the spectrum at the level crossings is expected to be described by a single CFT. As a consequence of conformal invariance, the scaling behaviour of the ground state energy is predicted to be [1, 9]

$$E = \epsilon_\infty \mathcal{L} - (c\, v_\mathrm{F}) \times \frac{\pi}{6\mathcal{L}} + o(\mathcal{L}^{-1}),$$

where c is the central charge of the underlying Virasoro algebra. For a given realization of the CFT its operator content is constrained by modular invariance of the partition function and the particular choice of boundary conditions [10, 11]. Further constraints are imposed by locality of the physical fields. The primary fields present in the critical model determine the finite-size energies and partial momenta of the excitated states:

$$E(\mathcal{L}) - E_0(\mathcal{L}) = \frac{2\pi\, v_\mathrm{F}}{\mathcal{L}}\,(X + n + \bar{n})\,, \qquad P(\mathcal{L}) - P_0(\mathcal{L}) = \frac{2\pi}{\mathcal{L}}\,(s + n - \bar{n}) + \mathrm{const.} \tag{29}$$

This allows us to determine the scaling dimensions $X = h + \bar{h}$ and conformal spins $s = h - \bar{h}$ of the primary fields (n, $\bar{n}$ are non-negative integers) from numerical finite-size data obtained by solution to the Bethe equations along with equations (11) and (13). Note that due to the massive degeneracies appearing in the spectrum for couplings θ being integer multiples of $\pi/2$ the complete momenta are not unique. The partial ones entering (29), however, are. This allows the use of finite-size data at the level crossings for the identification of the critical theory.

4.1.1. Spectrum of $\mathcal{H}_{\theta=\pi}$. The ground state energy of $\mathcal{H}_{\theta=\pi}$ is known to be [3, 24]

$$E_0 = -\left[\frac{1}{\pi} + \frac{2\sqrt{3}}{9}\right]\mathcal{L} - \frac{12}{5} \times \frac{\pi}{6\mathcal{L}} + o(\mathcal{L}^{-1}). \tag{30}$$

Using the Fermi-velocity (27) computed before the central charge of the effective field theory for the low energy degrees of freedom in $\mathcal{H}_{\theta=\pi}$ is identified to be $c = 4/5$. Hence, this sector of the model is in the universality class of the minimal model $\mathcal{M}_{(5,6)}$ and the conformal weights h, $\bar{h}$ of the primary fields can take the rational values from the Kac table

$$h, \bar{h} \in \left\{ \frac{(6p-5q)^2 - 1}{120} \,\middle|\, 1 \leqslant q \leqslant p < 5 \right\} = \left\{0, \frac{1}{40}, \frac{1}{15}, \frac{1}{8}, \frac{2}{5}, \frac{21}{40}, \frac{2}{3}, \frac{7}{5}, \frac{13}{8}, 3\right\}.$$

To identify the operator content of the periodic spin chain we have solved the Bethe equations (10) for lattice sizes up to a minimum of $\mathcal{L} = 40$, although over 100 sites were considered whenever possible. The sequence of finite-size estimations for the scaling dimensions

$$X_\theta^{\mathrm{num}}(\mathcal{L}) = \frac{\mathcal{L}}{2\pi\, v_\mathrm{F}}\,(E(\mathcal{L}) - E_0(\mathcal{L}))$$

Table 1. Scaling dimensions X_π extrapolated from the finite-size behaviour of the ground state and low-energy excitations of $\mathcal{H}_{\theta=\pi}$ (periodic) for even $\mathcal{L}$. $(h, \bar{h})$ are the predictions from the $\mathcal{M}_{(5,6)}$ minimal model. We have also indicated the $D(D_3)$ sector in which the state appears and its conjectured degeneracy. The operator content of the sector $\pi_\mathfrak{d}$ is obtained from that of $\pi_\mathfrak{c}$ by interchanging h and $\bar{h}$.

$D(D_3)$	$X_\pi^{\text{ext.}}$	$(h, \bar{h})$	Spin	Degeneracy
$\pi_\mathfrak{a} \oplus \pi_\mathfrak{b}$	0.000 000(1)	$(0, 0)$	0	$1 \times 3^{\frac{\mathcal{L}}{2}-1}$
	0.801(3)	$(\frac{2}{5}, \frac{2}{5})$	0	$1 \times 3^{\frac{\mathcal{L}}{2}-1}$
	1.80(1)	$(\frac{2}{5}, \frac{7}{5}), (\frac{7}{5}, \frac{2}{5})$	± 1	$1 \times 3^{\frac{\mathcal{L}}{2}-1}$
$\pi_\mathfrak{c}$	0.4668(2)	$(\frac{1}{15}, \frac{2}{5})$	$-\frac{1}{3}$	$2 \times 3^{\frac{\mathcal{L}}{2}-1}$
	0.666 666(1)	$(\frac{2}{3}, 0)$	$\frac{2}{3}$	$2 \times 3^{\frac{\mathcal{L}}{2}-1}$
$\pi_\mathfrak{e} \oplus \pi_\mathfrak{f}$	0.133 34(6)	$(\frac{1}{15}, \frac{1}{15})$	0	$4 \times 3^{\frac{\mathcal{L}}{2}-1}$
	1.333 33(3)	$(\frac{2}{3}, \frac{2}{3})$	0	$4 \times 3^{\frac{\mathcal{L}}{2}-1}$

has then be extrapolated to get a numerical approximation $X_\theta^{\text{ext.}}$ to the scaling dimension which can then be identified with a pair $(h, \bar{h})$ of conformal weights from the Kac table. In table 1 we present our data for the low-lying excitations appearing in the $\theta = \pi$ sector of the periodic spin chain for even chain lengths.

For the analysis of the finite-size spectrum, it is convenient to classify excitations of the model in terms of symmetry sectors. For even $\mathcal{L}$ the Hilbert space of the spin chain can be decomposed as

$$\pi_\mathfrak{g}^{\otimes\mathcal{L}} = \tfrac{1}{2}(3^{\mathcal{L}-2}+1)\pi_\mathfrak{a} \oplus \tfrac{1}{2}(3^{\mathcal{L}-2}-1)\pi_\mathfrak{b} \oplus 3^{\mathcal{L}-2}\left[\pi_\mathfrak{c} \oplus \pi_\mathfrak{d} \oplus \pi_\mathfrak{e} \oplus \pi_\mathfrak{f}\right].$$

However, as periodic closure of the system breaks the $D(D_3)$ invariance of the model we can no longer use this decomposition directly. Instead, we find it useful to define four residual symmetry sectors, i.e. $\pi_\mathfrak{a} \oplus \pi_\mathfrak{b}$, $\pi_\mathfrak{c}$, $\pi_\mathfrak{d}$ and $\pi_\mathfrak{e} \oplus \pi_\mathfrak{f}$. Here, the symmetry sector $\pi_\mathfrak{a} \oplus \pi_\mathfrak{b}$ is defined to be the subspace of $\pi_\mathfrak{g}^{\otimes\mathcal{L}}$ composed of all one-dimensional irreps ($\pi_\mathfrak{a}$ and $\pi_\mathfrak{b}$) appearing in its decomposition, likewise for the other sectors. Under this definition we find that all of these (non-intersecting) symmetry sectors are invariant under the action of global Hamiltonian of the periodic spin chain with generic θ.

Apart from fixing transformation properties of the excited states their classification according to symmetry counting arguments can be used to conjecture the degeneracy of each excitation for large finite systems based on the finite-size spectra, also shown in table 1. Furthermore, it has been noticed [23] that the symmetry of the eigenstates is connected to the number of Bethe roots at $\pm\infty$, see table 2. Finally, we observe that every excitation $(h, \bar{h})$ appearing in the sector $\pi_\mathfrak{c}$ can be related to an excitation $(\bar{h}, h)$ appearing in sector $\pi_\mathfrak{d}$ via a mapping of Bethe roots, $\{x_j\} \to \{-x_j\}$.

The excitations appearing here for even $\mathcal{L}$ coincide with those from the self-dual ferromagnetic three-state Potts quantum chain subjected to either periodic of twisted boundary conditions [61]. This stems from both models being constructed from the same set of solutions to the star-triangle equation [19], albeit with different limits applied. The excitations in the $\pi_\mathfrak{a} \oplus \pi_\mathfrak{b}$ and $\pi_\mathfrak{e} \oplus \pi_\mathfrak{f}$ sectors have been observed in the charge $Q = 0$ and 1 sector of the periodic

Table 2. The classification of symmetry sectors of the periodic spin chain in terms of the number of finite and infinite Bethe roots for chains of even length.

Symmetry sector	$N_- + N_+ + 2N_s$	$n_{-\infty}$	$n_{+\infty}$
$\pi_{\mathfrak{a}} \oplus \pi_{\mathfrak{b}}$	$\mathcal{L}$	0	0
$\pi_{\mathfrak{c}}$	$\mathcal{L}-1$	0	1
$\pi_{\mathfrak{d}}$	$\mathcal{L}-1$	1	0
$\pi_{\mathfrak{e}} \oplus \pi_{\mathfrak{f}}$	$\mathcal{L}-2$	1	1

Table 3. As table 1 for $\mathcal{H}_{\theta=\pi}$ (periodic) when is $\mathcal{L}$ odd. Symmetry is classified by the action of the D_3 rotation σ.

σ	$X_\pi^{\text{ext.}}$	$(h, \bar{h})$	Spin	Degeneracy
1	0.125 000(5)	$(0, \frac{1}{8})$	$-\frac{1}{8}$	$1 \times 3^{\frac{\mathcal{L}-1}{2}}$
	0.425 02(2)	$(\frac{2}{5}, \frac{1}{40})$	$\frac{3}{8}$	$1 \times 3^{\frac{\mathcal{L}-1}{2}}$
	0.924 90(6)	$(\frac{2}{5}, \frac{21}{40})$	$-\frac{1}{8}$	$1 \times 3^{\frac{\mathcal{L}-1}{2}}$
	1.625 000(1)	$(0, \frac{13}{8})$	$-\frac{13}{8}$	$1 \times 3^{\frac{\mathcal{L}-1}{2}}$
ω, ω^{-1}	0.091 665(2)	$(\frac{1}{15}, \frac{1}{40})$	$\frac{1}{24}$	$2 \times 3^{\frac{\mathcal{L}-1}{2}}$
	0.591 68(7)	$(\frac{1}{15}, \frac{21}{40})$	$-\frac{11}{24}$	$2 \times 3^{\frac{\mathcal{L}-1}{2}}$
	0.791 667(1)	$(\frac{2}{3}, \frac{1}{8})$	$\frac{13}{24}$	$2 \times 3^{\frac{\mathcal{L}-1}{2}}$

Table 4. The symmetry sectors of the periodic spin chain classified in terms of the number of finite and infinite Bethe roots for chains of odd length.

Symmetry sector	$N_- + N_+ + 2N_s$	$n_{-\infty}$	$n_{+\infty}$
1	$\mathcal{L}$	0	0
ω, ω^{-1}	$\mathcal{L}-1$	0	1

three-state Potts chain, respectively. The excitations in the $\pi_{\mathfrak{c}}$ and $\pi_{\mathfrak{d}}$ sectors correspond to the three-state Potts chain with twisted boundary conditions allowing for the non-half-integer spins observed. The excitations appearing in the periodic Potts chain have also been determined using Bethe ansatz methods by Albertini *et al* [3].

We have also determined the excitations for chains of odd length. In this case the states can be classified by the eigenvalue of the state under the D_3 rotation operator, σ. The excitations are given in table 3.

These excitations are not present in the three-state Potts model since the equivalence to this model is restricted to $\mathcal{L}$ even. We were able to again classify the symmetry sectors in terms of Bethe roots as presented in table 4. We found that $n_{-\infty} = 0$ in the case of odd length chains.

4.1.2. Spectrum of $\mathcal{H}_{\theta=0}$. The ground state energy is known to be [3, 24]

$$E_0 = -\left[\frac{1}{2\pi} - \frac{2\sqrt{3}}{9} + \frac{3}{4}\right]\mathcal{L} - \frac{3}{2} \times \frac{\pi}{6\mathcal{L}} + o(\mathcal{L}^{-1}). \tag{31}$$

Table 5. Scaling dimensions X_0 extrapolated from the finite-size behaviour of the ground state and low energy excitations of $\mathcal{H}_{\theta=0}$ (periodic) for $\mathcal{L} = 0 \pmod 4$ (the error of the extrapolation is smaller than the last displayed digit). $(h, \bar{h})$ are the predictions from the Z_4 parafermionic CFT. For the other columns, see table 1.

$D(D_3)$	$X_0^{\text{ext.}}$	$(h, \bar{h})$	Spin	Degeneracy
$\pi_{\mathfrak{a}} \oplus \pi_{\mathfrak{b}}$	0.000 000	$(0, 0)$	0	$1 \times 3^{\frac{\mathcal{L}}{2}-1}$
$\pi_{\mathfrak{c}}$	0.333 332	$(0, \frac{1}{3})$	$-\frac{1}{3}$	$2 \times 3^{\frac{\mathcal{L}}{2}-1}$
$\pi_{\mathfrak{e}} \oplus \pi_{\mathfrak{f}}$	0.166 667	$(\frac{1}{12}, \frac{1}{12})$	0	$4 \times 3^{\frac{\mathcal{L}}{2}-1}$
	0.666 667	$(\frac{1}{3}, \frac{1}{3})$	0	$4 \times 3^{\frac{\mathcal{L}}{2}-1}$

Table 6. As table 5 for $\mathcal{H}_{\theta=0}$ (periodic) when $\mathcal{L} = 1 \pmod 4$. The excitations for chains with length $\mathcal{L} = 3 \pmod 4$ have the same exponents but the opposite spin. Symmetry is classified by the action of the D_3 rotation σ.

σ	$X_0^{\text{ext.}}$	$(h, \bar{h})$	Spin	Degeneracy
1	0.062 500	$(\frac{1}{16}, 0)$	$\frac{1}{16}$	$1 \times 3^{\frac{\mathcal{L}-1}{2}}$
	0.562 500	$(\frac{9}{16}, 0)$	$\frac{9}{16}$	$1 \times 3^{\frac{\mathcal{L}-1}{2}}$
	0.812 500	$(\frac{1}{16}, \frac{3}{4})$	$-\frac{11}{16}$	$1 \times 3^{\frac{\mathcal{L}-1}{2}}$
ω, ω^{-1}	0.145 833	$(\frac{1}{16}, \frac{1}{12})$	$-\frac{1}{48}$	$2 \times 3^{\frac{\mathcal{L}-1}{2}}$
	0.395 833	$(\frac{1}{16}, \frac{1}{3})$	$-\frac{13}{48}$	$2 \times 3^{\frac{\mathcal{L}-1}{2}}$
	0.645 833	$(\frac{9}{16}, \frac{1}{12})$	$\frac{23}{48}$	$2 \times 3^{\frac{\mathcal{L}-1}{2}}$

Using the Fermi velocity we find that the central charge is 1, which does not uniquely define a CFT. The field content of the theory is obtained from the finite-size spectrum. One method of determining the finite-size spectrum is using the dressed charge formalism (see the appendix) leading to the identification of the Z_4 parafermion theory [29, 64] coinciding with the anti-ferromagnetic three-state Potts model. The allowed conformal weights for this theory are [29, 47]

$$h, \bar{h} \in \left\{ \frac{l(l+2)}{24} - \frac{m^2}{16} \middle| 0 \leqslant m \leqslant l \leqslant 4,\ l \equiv m \pmod 2 \right\} = \left\{ 0, \frac{1}{16}, \frac{1}{12}, \frac{1}{3}, \frac{9}{16}, \frac{3}{4}, 1 \right\}.$$

Alternately, we can solve the Bethe equations directly and determine the scaling behaviour of the low-lying excitations. Here we must consider $\mathcal{L} = 0, 1, 2, 3 \pmod 4$ separately, see tables 5–7 below. In particular, we find that the finite-size gap of the lowest states for $\ell = \mathcal{L} \pmod 4 \neq 0$ is determined by an (anti-)chiral $Z_{k=4}$ spin field with conformal weight $h_\ell = \ell(k-\ell)/(2k(k+2))$.

As with the previous case we again can partition the excitations according to the residual symmetry sectors. These sectors are still characterized by the number of Bethe roots at $\pm\infty$ as described in table 2.

Table 7. As table 5 but for $\mathcal{H}_{\theta=0}$ (periodic) when $\mathcal{L} = 2 \pmod 4$.

$D(D_3)$	$X_0^{\text{ext.}}$	$(h, \bar{h})$	Spin	Degeneracy
$\pi_{\mathfrak{a}} \oplus \pi_{\mathfrak{b}}$	0.750 000	$(0, \frac{3}{4}) \times 2$, $(\frac{3}{4}, 0) \times 2$	$\pm\frac{3}{4}$	$1 \times 3^{\frac{\mathcal{L}}{2}-1}$
$\pi_{\mathfrak{c}}$	0.083 333	$(0, \frac{1}{12})$	$-\frac{1}{12}$	$2 \times 3^{\frac{\mathcal{L}}{2}-1}$
	1.083 333	$(\frac{3}{4}, \frac{1}{3})$	$\frac{5}{12}$	$2 \times 3^{\frac{\mathcal{L}}{2}-1}$
$\pi_{\mathfrak{e}} \oplus \pi_{\mathfrak{f}}$	0.416 667	$(\frac{1}{12}, \frac{1}{3}), (\frac{1}{3}, \frac{1}{12})$	$\pm\frac{1}{4}$	$4 \times 3^{\frac{\mathcal{L}}{2}-1}$

Table 8. The pairing multiplicities, m_p, of the periodic spin chain for any two energies of $\mathcal{H}^{(1)}$ and $\mathcal{H}^{(2)}$ that belong to the same symmetry sector. If the energies do not belong to the same symmetry sector then they do not pair, i.e. the pairing multiplicity is zero.

	$\mathcal{L} = 0 \pmod 2$			$\mathcal{L} = 1 \pmod 2$		
Sector	$\pi_{\mathfrak{a}} \oplus \pi_{\mathfrak{b}}$	$\pi_{\mathfrak{c}}$	$\pi_{\mathfrak{d}}$	$\pi_{\mathfrak{e}} \oplus \pi_{\mathfrak{f}}$	1	w, w^{-1}
m_p	1	2	2	4	1	2

Comparing these excitations to the anti-ferromagnetic three-state Potts chain [3, 47] (for $\mathcal{L}$ even), we find that the excitations in the $\pi_{\mathfrak{a}} \oplus \pi_{\mathfrak{b}}$ and $\pi_{\mathfrak{e}} \oplus \pi_{\mathfrak{f}}$ were previously identified and restricted to the $n_{+\infty} = n_{-\infty}$ case. We were unable to find any literature dealing with the anti-ferromagnetic end of the twisted three-Potts model. We expect, however, that the excitations in that case to match those appearing in the $\pi_{\mathfrak{c}}$ and $\pi_{\mathfrak{d}}$ sectors. Similarly the excitations for odd $\mathcal{L}$ have not previously been studied.

4.1.3. Pairing rules and discussion. The results on the low-energy spectra $\mathcal{H}_\theta$ for $\theta = 0, \pi$ completely determine the critical behaviour (up to degeneracies) of the periodic $D(D_3)$ spin chain at all the level crossings, i.e. when θ is a multiple of $\frac{\pi}{2}$: this is a consequence of the fact that the partial energies, i.e. eigenvalues (11) of $\mathcal{H}^{(1)}$ and $\mathcal{H}^{(2)}$, and momenta (13) corresponding to a given Bethe root configuration are identical (although the partial momenta enter in the definition of the total momentum (14) with opposite signs).

For generic values of θ the energy eigenvalues of the periodic spin chain are given by (12) in terms of two root configurations of the Bethe equations (10) provided that these configurations pair. Based on studies of small system sizes, it has been observed that two sets of Bethe roots pair to form an eigenvalue of the transfer matrix, equation (8), if and only if they have matching number of roots at $\pm\infty$ [24]. As a consequence of the classification of excitations according to their symmetry above, see tables 2 and 4, this is equivalent to saying Bethe root configurations (and their corresponding energies) pair if and only if they belong to the same symmetry sector. Furthermore, we have observed that within a symmetry sector pairing is uniform in the sense that every two sets of Bethe root configurations within a symmetry sector pair the same number of times, a quantity referred to as the pairing multiplicity. The relationship between pairing multiplicity and symmetry sectors is documented in table 8.

This information, along with equations (12) and (29) and the relevant tables, is sufficient to determine the energies and degeneracies of the ground state and low-lying excitations

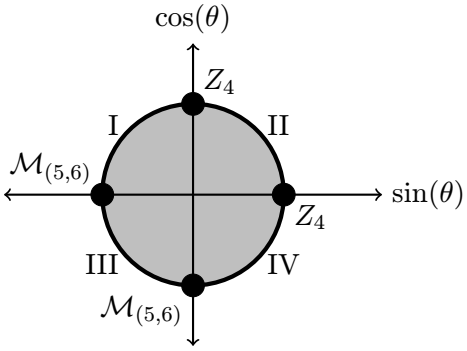

Figure 3. CFT description of the periodic integrable $D(D_3)$ symmetric model for generic θ. Level crossing are described by minimal models, either Z_4 parafermions or $\mathcal{M}_{(5,6)}$, while the regions in between are described by a product of the theories of the two adjacent level crossings. Therefore regions I and IV correspond to a $Z_4 \otimes \mathcal{M}_{(5,6)}$ theory, while regions II and III correspond, respectively, to $Z_4 \otimes Z_4$ and $\mathcal{M}_{(5,6)} \otimes \mathcal{M}_{(5,6)}$ theories.

of the model for generic θ. The resulting spectrum is that of a direct product of two conformal field theories. The physical fields appearing in the combined theory are composite operators with scaling dimension $X_{\rm tot} = X^{(1)} + X^{(2)} = \sum_{k=1}^{2}(h^{(k)} + \bar{h}^{(k)})$ with $(h^{(k)}, \bar{h}^{(k)})$ being the conformal weights from the two components. Similarly, the total spin of an excitation can be calculated from equations (14) and (29) giving $s_{\rm tot} = s^{(1)} - s^{(2)} = h^{(1)} - \bar{h}^{(1)} - h^{(2)} + \bar{h}^{(2)}$. Note that application of the pairing rules to the conformal dimensions identified for the periodic spin chain above ensure that this total spin is always either an integer or half-integer which guarantees locality of the physical fields.

The phase diagram of the complete model can be summarized by figure 3.

4.2. Periodic fusion path chain

By construction this chain differs from the periodic spin chain discussed in the previous section only through boundary conditions. Therefore, the two models share their bulk properties, including energy per unit lattice site, Fermi velocity and central charge. To identify the operator content of the low-energy effective theory for the fusion path model, we have computed the complete spectrum of the Hamiltonian numerically for up to $\mathcal{L} = 10$ sites. We find that part of the spectrum coincides (numerically exact) with eigenvalues of the periodic spin chain (although the corresponding degeneracies in the different formalisms do not match). Specifically, this applies to the energies that have been associated with the $\pi_{\mathfrak{a}} \oplus \pi_{\mathfrak{b}}$ and $\pi_{\mathfrak{e}} \oplus \pi_{\mathfrak{f}}$ symmetry sectors above (we emphasize that the periodic fusion path model can only be constructed for $\mathcal{L}$ even). In addition, we have diagonalized the transfer matrix for up to $\mathcal{L} = 8$ sites. From these results we find that the transfer matrix eigenvalues factorize into two polynomials as in (8). The corresponding roots of these polynomials can be used to parametrize the eigenvalues and are conjectured to be given by the Bethe equations (22).

We have verified this conjecture by comparing the energies obtained from the Bethe equations with those obtained by numerical diagonalization. The eigenvalues appearing in both the spin chain and the fusion path formalism are described by root configurations

Table 9. Scaling dimensions X_π extrapolated from the finite-size behaviour of the ground state and low-energy excitations of $\tilde{\mathcal{H}}_{\theta=\pi}$ (fusion path) for $\mathcal{L} = 0 \pmod 2$. From the numerical diagonalization of the Hamiltonian for finite-size systems, we conjecture the degeneracy of each pair of conformal weights, $(h, \bar{h})$. The value η is from the Bethe equations (22).

$X_\pi^{\text{ext.}}$	$(h, \bar{h})$	Spin	Degeneracy	η
0.000 000(1)	$(0, 0)$	0	$\frac{1}{2}(3^{\frac{\mathcal{L}}{2}}+1)$	+1
0.050 04(5)	$(\frac{1}{40}, \frac{1}{40})$	0	$\frac{1}{2}(3^{\frac{\mathcal{L}}{2}}+1)$	−1
0.133 34(4)	$(\frac{1}{15}, \frac{1}{15})$	0	$3^{\frac{\mathcal{L}}{2}}$	+1
0.250 01(3)	$(\frac{1}{8}, \frac{1}{8})$	0	$\frac{1}{2}(3^{\frac{\mathcal{L}}{2}}+1)$	−1
0.549(2)	$(\frac{1}{40}, \frac{21}{40}), (\frac{21}{40}, \frac{1}{40})$	$\pm\frac{1}{2}$	$\frac{1}{2}(3^{\frac{\mathcal{L}}{2}}-1)$	−1
0.801(3)	$(\frac{2}{5}, \frac{2}{5})$	0	$\frac{1}{2}(3^{\frac{\mathcal{L}}{2}}+1)$	+1
1.06(2)	$(\frac{21}{40}, \frac{21}{40})$	0	$\frac{1}{2}(3^{\frac{\mathcal{L}}{2}}+1)$	−1
1.333 33(3)	$(\frac{2}{3}, \frac{2}{3})$	0	$3^{\frac{\mathcal{L}}{2}}$	+1
1.80(1)	$(\frac{2}{5}, \frac{7}{5}), (\frac{7}{5}, \frac{2}{5})$	±1	$\frac{1}{2}(3^{\frac{\mathcal{L}}{2}}-1)$	+1

solving (22) with $\eta = +1$. This includes the ground states of $\mathcal{H}_{\theta=\pi}$ and $\mathcal{H}_{\theta=0}$ with energies given by equations (30) and (31), respectively. Generally, we find that each set of Bethe roots corresponding to an eigenvalue of the periodic fusion path chain contains either only finite roots or, for $\eta = +1$, exactly two roots at $+\infty$ and $-\infty$.

4.2.1. Spectrum of $\tilde{\mathcal{H}}_{\theta=\pi}$. As this model shares bulk properties with the periodic spin chain this model lies in the $M_{(5,6)}$ universality class with central charge $c = \frac{4}{5}$. From the diagonalization of the transfer matrix we can associate root configurations to the ground state and low-lying excitations of $\tilde{\mathcal{H}}_{\theta=\pi}$ which consist of $\approx\frac{1}{2}\mathcal{L}$ two-strings and a few $\pm$-strings. Solving the conjectured Bethe equations for systems of up to 100 sites, we have found the excitations given in table 9.

Note that the new excitations corresponding to roots of the Bethe equations (22) with $\eta = -1$ do not correspond to excitations of the three-state Potts chains subject to the boundary conditions studied previously [61]. Moreover, because the formulation of this chain is reliant on $D(D_3)$ symmetry, which is not present in the usual three-state Potts local Hamiltonian, it is reasonable to expect that these excitations will not appear for any other formulation of the three-state Potts model.

4.2.2. Spectrum of $\tilde{\mathcal{H}}_{\theta=0}$. Using similar methods we can determine the low-energy excitations of the fusion path model for $\theta = 0$. This is done for even $\mathcal{L}$ where, as in the spin chain case, we have to discuss the cases of $\frac{\mathcal{L}}{2}$ even or odd separately. The conformal dimensions identified from the low-lying excitations are shown in table 10.

As was the case with the $\tilde{\mathcal{H}}_{\theta=\pi}$ model we find new excitations, again characterized by $\eta = -1$, which do not appear in three-state Potts chains subject to the boundary conditions studied previously. Due to commensurability conditions the spectra can only be compared for

Table 10. Scaling dimensions X_0 extrapolated from the finite-size behaviour of the ground state and low-energy excitations of $\tilde{\mathcal{H}}_{\theta=0}$ (fusion path) for $\mathcal{L} = 0, 2 \pmod 4$. We have omitted the column regarding the degeneracy of the excitation due to a lack of data. The error of the extrapolation is smaller than the last displayed digit. The association of a $\times 2$ with a pair of conformal weights implies that there are two excitations with those conformal weights that have distinct energies for finite-size systems.

$\mathcal{L} \bmod 4$	$X_0^{\text{ext.}}$	$(h, \bar{h})$	Spin	η
0	0.000 000	$(0, 0)$	0	+1
	0.125 000	$(\frac{1}{16}, \frac{1}{16})$	0	−1
	0.166 667	$(\frac{1}{12}, \frac{1}{12})$	0	+1
	0.625 000	$(\frac{9}{16}, \frac{1}{16}) \times 2$, $(\frac{1}{16}, \frac{9}{16}) \times 2$	$\pm\frac{1}{2}$	−1
	0.666 667	$(\frac{1}{3}, \frac{1}{3})$	0	+1
2	0.125 000	$(\frac{1}{16}, \frac{1}{16}) \times 2$	0	−1
	0.416 667	$(\frac{1}{3}, \frac{1}{12}), (\frac{1}{12}, \frac{1}{3})$	$\pm\frac{1}{4}$	+1
	0.625 000	$(\frac{9}{16}, \frac{1}{16}) \times 2$, $(\frac{1}{16}, \frac{9}{16}) \times 2$	$\pm\frac{1}{2}$	−1
	0.750 000	$(0, \frac{3}{4}) \times 2$, $(\frac{3}{4}, 0) \times 2$	$\pm\frac{3}{4}$	+1

lattices with lengths differing by multiples of 4. Therefore, we do not have sufficient numerical data from exact diagonalization of the Hamiltonian to present any conjectures concerning the degeneracy of the excitations.

4.2.3. Pairing rules and discussion. In contrast to the periodic spin formulation the pairing rules for the periodic fusion path chain could not be easily determined. The residual symmetry sectors used in the previous section are no longer present. It is possible, however, to define a conserved topological charge for the fusion path model based on the $D(D_3)$ F-moves aforementioned [20, 30]. This charge allows us to differentiate between different topological sectors which are labelled by the irreps of $D(D_3)$. A better understanding of these topological symmetry sectors will be necessary to gain insight into the pairing rules for this model.

Finally, we want to stress that while the computation of scaling dimensions is based on the solution of the Bethe equations (22), which can be achieved for relatively large $\mathcal{L}$, the identification of allowed Bethe root configurations still relied upon the explicit diagonalization of the transfer matrices of small systems. Thus while we have a high level of confidence in the accuracy of the scaling dimension it is not clear whether all primary excitations have been identified. In particular, the existence of additional primary operators with larger scaling dimensions cannot be ruled out.

4.3. Braided chain

As discussed above, the $D(D_3)$ quantum chains in the spin chain and the fusion path formalism are equivalent for braided and open boundary conditions. Therefore we discuss their critical properties in the former.

4.3.1. Spectrum of $\mathcal{H}_{\theta=\pi}$. The full spectrum of the $\mathcal{H}_{\theta=\pi}$ braided chain is a subset of the spectrum of the $\mathcal{H}_{\theta=\pi}$ periodic spin chain. In particular we find that, for the choice of the braiding operator used in this work, the energies present are those that appeared in the symmetry sectors $\pi_{\mathfrak{a}} \oplus \pi_{\mathfrak{b}}$ and $\pi_{\mathfrak{c}}$ of the periodic chain for even $\mathcal{L}$ and in the $\sigma = 1$ for odd $\mathcal{L}$. As a consequence, only Bethe root configurations with $n_{-\infty} = 0$ for even length chains ($n_{\pm\infty} = 0$ for odd length chains) correspond to eigenvalues of the braided model. Therefore, the low-lying excitations for the braided chain can be deduced from tables 1 and 3:

$$(h, \bar{h}) \in \begin{cases} \left\{(0,0), (\frac{2}{5}, \frac{2}{5}), (\frac{2}{5}, \frac{7}{5}), (\frac{7}{5}, \frac{2}{5}), (\frac{1}{15}, \frac{2}{5}), (\frac{2}{3}, 0)\right\}, & \mathcal{L} \quad \text{even}, \\ \left\{(0, \frac{1}{8}), (\frac{2}{5}, \frac{1}{40}), (\frac{2}{5}, \frac{21}{40}), (0, \frac{13}{8})\right\}, & \mathcal{L} \quad \text{odd}. \end{cases}$$

Since the braided chain has the full $D(D_3)$ symmetry it would be possible to classify all eigenstates of this model in terms of the irreps. We find, however, that the enlarged symmetry gives rise to additional degeneracies in the spectrum which extend across multiple symmetry sectors of the braided spin chain. This implies that for these boundary conditions a classification of symmetry sectors based on the presence of infinite Bethe roots is no longer possible. In particular, this leads to higher degeneracies in the spectrum of the braided spin chain model as compared to the periodic one.

4.3.2. Spectrum of $\mathcal{H}_{\theta=0}$. As $\mathcal{H}_{\theta=0} = -\mathcal{H}_{\theta=\pi}$ we can again use our results for the periodic spin chain to discuss the low-energy spectrum of the braided one. Just as for $\theta = \pi$ the excitations appearing in the braided chain are those present in the $\pi_{\mathfrak{a}} \oplus \pi_{\mathfrak{b}}$ and $\pi_{\mathfrak{c}}$ sectors of the periodic chain for even $\mathcal{L}$ and in the $\sigma = 1$ sector for odd $\mathcal{L}$. Thus, we can deduce the excitations appearing in the braided model from tables 5–7:

$$(h, \bar{h}) \in \begin{cases} \left\{(0,0), (0, \frac{1}{3})\right\}, & \mathcal{L} \equiv 0 \mod 4, \\ \left\{(\frac{1}{16}, 0), (\frac{9}{16}, 0), (\frac{1}{16}, \frac{3}{4})\right\}, & \mathcal{L} \equiv 1 \mod 4, \\ \left\{(0, \frac{3}{4}), (\frac{3}{4}, 0), (0, \frac{1}{12}), (\frac{3}{4}, \frac{1}{3})\right\}, & \mathcal{L} \equiv 2 \mod 4, \\ \left\{(\frac{1}{16}, 0), (\frac{9}{16}, 0), (\frac{1}{16}, \frac{3}{4})\right\}, & \mathcal{L} \equiv 3 \mod 4. \end{cases}$$

4.3.3. Pairing rules and discussion. Like the periodic case the results for the braided chain at $\theta = 0, \pi$ determine the low-energy spectrum at all of the level crossings. Again, the full spectrum for generic θ is given by (12) in terms of two Bethe root configurations provided that these configurations pair. For the braided model it has been observed previously that any two solutions to the Bethe equations can be paired to form an eigenvalue of the transfer matrix given by equation (8) [24]. This is consistent with statement above, that a given root configuration corresponds to eigenstates in multiple symmetry sectors. Another difference to the periodic spin chain is that the assignment of a root configuration to a particular symmetry sector of the braided chain is different for $\mathcal{H}^{(1)}$ or $\mathcal{H}^{(2)}$. Despite these technical differences we find that the pairing multiplicities, i.e. the number of times two solutions to the Bethe equations pair, depends solely on the symmetry sector the eigenvalue of the transfer matrix lies in and is defined by table 8.

Table 11. Conformal weights h extrapolated from the finite-size behaviour of the ground state and low-energy excitations of $\mathcal{H}_{\theta=\pi}$ (open) for different chain lengths. The expression for the degeneracy of the energy is written for easy comparison to table 1.

$\mathcal{L}$ mod 2	$h^{\text{ext.}}$	h	Degeneracy
0	0.000 000(1)	0	$3 \times 3^{\frac{\mathcal{L}}{2}-1}$
	0.666(1)	$\frac{2}{3}$	$6 \times 3^{\frac{\mathcal{L}}{2}-1}$
1	0.125(2)	$\frac{1}{8}$	$3 \times 3^{\frac{\mathcal{L}-1}{2}}$
	1.624(3)	$\frac{13}{8}$	$3 \times 3^{\frac{\mathcal{L}-1}{2}}$

As before, pairing determines the physical fields appearing in the low-energy effective theory of the braided spin chain. Their scaling dimensions and total spin of these composite operators are related to the ones of their components as before. We note, however, that the total momentum in the braided model is not a multiple of $2\pi/\mathcal{L}$ but instead constrained by equation (15).

4.4. Open chain

As in the case of braided boundary conditions it is sufficient to discuss the low-energy behaviour of the open chain in the spin chain formulation. At level crossings conformal invariance predicts that the lowest energies of the open chain with free ends, i.e. $\chi_1^{\pm} = \chi_2^{\pm} = 0$, have the scaling behaviour given by [9]

$$E = \epsilon_\infty \mathcal{L} + f_0 + \frac{\pi v_{\text{F}}}{\mathcal{L}} \left(-\frac{c}{24} + h + n \right) + o(\mathcal{L}^{-1}),$$

where c is the central charge, v_{F} is the Fermi-velocity, h is a conformal weight and n is a non-negative integer.

4.4.1. Spectrum of $\mathcal{H}_{\theta=\pi}$. The ground state energy for $\theta = \pi$ [24] is

$$E_0 = -\left[\frac{1}{\pi} + \frac{2\sqrt{3}}{9} \right] \mathcal{L} + \left[\frac{3}{2} - \frac{2\sqrt{3}}{3} \right] - \frac{12}{5} \times \frac{\pi}{24\mathcal{L}} + o(\mathcal{L}^{-1}).$$

As is the case with the periodic chain we have that $v_{\text{F}} = 3$ and $c = \frac{4}{5}$, yielding the same CFT as expected. Using an analogous method to that outlined in section 4.1.1 to calculate $X^{\text{ext.}}$ we can extrapolate values for the conformal weights, $h^{\text{ext.}}$. The values are presented in table 11.

4.4.2. Spectrum of $\mathcal{H}_{\theta=0}$. The ground state of the open chain for $\theta = 0$ [24] is

$$E_0 = -\left[\frac{1}{2\pi} - \frac{2\sqrt{3}}{9} + \frac{3}{4} \right] \mathcal{L} + \left[-\frac{3}{4} + \frac{2\sqrt{3}}{3} \right] - \frac{3}{2} \times \frac{\pi}{24\mathcal{L}} + o(\mathcal{L}^{-1}),$$

which gives $v_{\text{F}} = \frac{3}{2}$ and $c = 1$, in agreement with the periodic chain. As with the previous section we numerically approximate the conformal weights by solving the Bethe equations. The results are summarized in table 12.

Table 12. Conformal weights h extrapolated from the finite-size behaviour of the ground state and low-energy excitations of $\mathcal{H}_{\theta=0}$ (open) for different chain lengths. The conformal weights appearing when $\mathcal{L} = 3 \pmod 4$ have been omitted as they are identical to the $\mathcal{L} = 1 \pmod 4$ case. As was the case with table 5 the error of the extrapolation is smaller than the last displayed digit.

$\mathcal{L}$ mod 4	$h^{\text{ext.}}$	h	Degeneracy
0	0.000 000	0	$3 \times 3^{\frac{\mathcal{L}}{2}-1}$
	0.333 333	$\frac{1}{3}$	$6 \times 3^{\frac{\mathcal{L}}{2}-1}$
	1.000 000	1	$3 \times 3^{\frac{\mathcal{L}}{2}-1}$
1	0.062 500	$\frac{1}{16}$	$3 \times 3^{\frac{\mathcal{L}-1}{2}}$
	0.562 500	$\frac{9}{16}$	$3 \times 3^{\frac{\mathcal{L}-1}{2}}$
2	0.083 333	$\frac{1}{12}$	$6 \times 3^{\frac{\mathcal{L}}{2}-1}$
	0.750 000	$\frac{3}{4}$	$3 \times 3^{\frac{\mathcal{L}}{2}-1}$
	0.750 000	$\frac{3}{4}$	$3 \times 3^{\frac{\mathcal{L}}{2}-1}$

We should remark that we have listed the conformal weight $h = \frac{3}{4}$ twice in table 12 to emphasize that there are two different Bethe root configurations with different finite-size energies extrapolating to this conformal dimension for $\mathcal{L} \mod 4 = 2$.

4.4.3. Pairing rules and discussion. This model is similar to the braided version and has the full global symmetry of the algebra $D(D_3)$. Every pair of solutions to the Bethe equations pair which again implies that conformal weights will appear in multiple symmetry sectors and the number of times they pair depends solely on the symmetry sector the eigenvalue of the transfer matrix lies in, table 8.

5. Discussion

In this paper we have analysed the low-energy spectrum of the integrable $D(D_3)$ symmetric chain subject to various boundary conditions. In the spin chain formulation the Hamiltonian derives from a commuting two-parameter transfer matrix of a vertex model and the eigenvalues can be obtained by Bethe ansatz methods. We have constructed a related class of models with local $D(D_3)$ symmetry using the fusion path formulation: these models, too, are integrable as they can be obtained from a solution to the Yang–Baxter equation for a face (or RSOS) model. For open and braided boundary conditions the two formulations of the model are equivalent. For periodic closure, however, the fusion path chain differs from the spin chain by boundary terms. Based on studies of small systems, we have proposed a set of Bethe equations whose solutions determine the eigenvalues of the fusion path chain.

From a finite-size analysis of the spectrum of these models, we have identified the conformal field theories providing an effective description of the low-energy modes to contain two sectors from—depending on the parameter θ—the minimal model $\mathcal{M}_{(5,6)}$ (the three-state Potts model) and the Z_4 parafermion. The physical fields are products of operators from these sectors. The individual factors can carry fractional (non-integer or non-(para)fermionic) spins

implying the appearance of Virasoro characters in the partition function of the model which have not been discussed in the context of $\mathcal{M}_{(5,6)}$ or Z_4 alone.

The locality of physical fields in the model is guaranteed by pairing rules. This situation is similar to other models with several gapless modes propagating with different Fermi velocities [8, 26, 27]. We have to emphasize, however, that in the present models this factorization of different modes is *exact* already for finite chains and on all energy scales, unlike in say the separation of spin and charge degrees of freedom observed within the low-energy spectrum of the one-dimensional Hubbard model where the coupling between the sectors becomes manifest in subleading corrections to scaling and at higher energies. Another difference for the model studied here is that the two sectors of the effective theory are not related to subalgebras of the global symmetry of the model. Therefore, to establish the pairing rules and corresponding multiplicities we have resorted to numerical studies of small systems together with counting arguments for the total number of states of the system. For the spin chain formulation we found that the pairing is determined by the boundary conditions and can be related to the residual symmetry of a given eigenstate. It is also reflected by the appearance of infinite roots appearing in the configurations solving the Bethe equations of the model. The spectrum of the periodic $D(D_3)$ model in the fusion path formulation also shows pairing on all energy scales. Unlike in the spin chain formulation, however, the pairing is not transitive and cannot be described based on residual symmetries as in the spin chain. The identification of the pairing rules and as to whether these rules are connected to topological invariants involving the $D(D_3)$ F-moves remains an interesting open problem for this model.

As a first step to address this problem, numerical methods could be used to form conjectures. Ultimately, however, it would be desirable to obtain the complete picture starting from the integrable structures underlying this model. For the topological invariants this requires to relate them to elements of the RSOS Yang–Baxter algebra. For the solution of the spectral problem of the anyon chain, the functional relations (21) have to be established using the fusion procedure for RSOS transfer matrices. We shall address these questions in future work.

Acknowledgments

We thank Jesper Romers for providing mathematica code that generated the F-moves for the $D(D_3)$ anyons, along with Karen Dancer, Fabian Essler, Jon Links and Robert Weston for discussing various topics relating to this paper and referring the authors to relevant literature. Parts of the numerical data used in this work have been obtained using the RRZN cluster system at Leibniz Universität Hannover. Support for this project by the Deutsche Forschungsgemeinschaft is gratefully acknowledged.

Appendix. Dressed charge formalism

Following [8, 18, 27, 58] the finite-size energy gaps of $\mathcal{H}_{\theta=0}$ for periodic boundary conditions are

$$\Delta E(\Delta N_{\pm}, Q_{\pm}) = \frac{2\pi}{\mathcal{L}} v_{\mathrm{F}} \Big(\frac{1}{4} (\Delta N_{+}, \Delta N_{-}) (\Xi^{\top} \Xi)^{-1} (\Delta N_{+}, \Delta N_{-}) + (Q_{+}, Q_{-}) (\Xi^{\top} \Xi) (Q_{+}, Q_{-}) + \mathcal{N} \Big) + o(\mathcal{L}^{-1}). \tag{A.1}$$

Table A.1. The lowest excitations of $\mathcal{H}_0$ in terms of the quantities $\Delta N_\pm$ and $Q_\pm$ for different chain lengths.

$\mathcal{L}$ mod 4	X	s	ΔN_+	ΔN_-	ΔQ_+	ΔQ_-
0	0	0	0	0	0	0
	$\frac{1}{3}$	$-\frac{1}{3}$	0	-1	$-\frac{1}{3}$	$+\frac{2}{3}$
	$\frac{2}{3}$	0	0	-2	0	0
	$\frac{1}{6}$	0	-1	-1	0	0
1	$\frac{1}{16}$	$\frac{1}{16}$	$-\frac{1}{4}$	$+\frac{1}{4}$	$+\frac{1}{4}$	$-\frac{1}{4}$
	$\frac{7}{48}$	$-\frac{1}{48}$	$-\frac{1}{4}$	$-\frac{3}{4}$	$-\frac{5}{12}$	$+\frac{1}{12}$
	$\frac{19}{48}$	$-\frac{13}{48}$	$-\frac{1}{4}$	$-\frac{3}{4}$	$+\frac{7}{12}$	$-\frac{11}{12}$
2	$\frac{1}{12}$	$-\frac{1}{12}$	$-\frac{1}{2}$	$-\frac{1}{2}$	$-\frac{1}{6}$	$-\frac{1}{6}$
	$\frac{5}{12}$	$-\frac{1}{4}$	$-\frac{1}{2}$	$-\frac{3}{2}$	$-\frac{1}{2}$	$+\frac{1}{2}$

($\mathcal{N}$ being a non-negative integer). Taking into account that only $\pm$-strings are present in the ground state the 2×2 dressed charge matrix $\Xi = \xi(x)|_{x=\infty}$ is obtained from the linear integral equation

$$\begin{aligned}\xi(x) &= \begin{pmatrix}1 & 0\\ 0 & 1\end{pmatrix} - \frac{1}{2\pi}\int_{-\infty}^{\infty} \mathrm{d}y\, \xi(y) K(y-x),\\ K(x) &= \begin{pmatrix}k(x,\frac{1}{3}) & k(x,\frac{5}{6})\\ k(x,\frac{5}{6}) & k(x,\frac{1}{3})\end{pmatrix}, \quad k(x,t) = \frac{\sin(2\pi t)}{\cosh(x)-\cos(2\pi t)}.\end{aligned} \tag{A.2}$$

Using Wiener Hopf techniques the dressed charge matrix can be expressed in terms of the Fourier transform of the kernel matrix giving

$$\Xi^{\top}\Xi = \left(1-\widetilde{K}(\omega=0)\right)^{-1} = \begin{pmatrix}1 & \frac{1}{2}\\ \frac{1}{2} & 1\end{pmatrix}. \tag{A.3}$$

Hence the scaling dimensions and conformal spins of primary operators in the effective field theory for $\mathcal{H}_{\theta=0}$ in terms of the quantum numbers $\Delta N_\pm$ and $Q_\pm$ characterizing the corresponding excitation (29) are

$$\begin{aligned}X &= \tfrac{1}{3}\left((\Delta N_+)^2 - \Delta N_+\Delta N_- + (\Delta N_-)^2\right) + \left((Q_+)^2 + Q_+Q_- + (Q_-)^2\right),\\ s &= -\tfrac{1}{2}\left(Q_+\Delta N_+ + Q_-\Delta N_-\right).\end{aligned} \tag{A.4}$$

The $\Delta N_\pm \equiv N_\pm - \frac{\mathcal{L}}{2} \pm \frac{\mathcal{L}}{4}$ correspond to the change in number of $\pm$-strings (subject to the condition that the total number of roots is $\mathcal{L}$) as compared to the thermodynamic ground state while the $Q_\pm$ determine the momentum of the excitation. For a configuration with $n_\pm$ Bethe roots at $\pm\infty$ they can take discrete values

$$Q_\pm \equiv \tfrac{1}{3}(n_{+\infty} - n_{-\infty}) \pmod 1.$$

For a given solution $\{x_k^\pm\}$ of the Bethe equations the $Q_\pm$ can also be determined numerically using the counting functions defined above:

$$Q_\pm = \frac{1}{N_\pm}\sum_{k=1}^{N_\pm} Z_\pm(x_k^\pm).$$

Due to the discrete set of possible values for $Q_{\pm}$ the data for systems with $\mathcal{L} \leqslant 10$ are sufficient to identify the quantum numbers for the lowest finite-size gaps of $\mathcal{H}_{\theta=0}$, see in table A.1. The observed dimensions support our identification of the critical theory with a Z_4 parafermion.

References

[1] Affleck I 1986 Universal term in the free energy at a critical point and the conformal anomaly *Phys. Rev. Lett.* **56** 746–748

[2] Albertini G, Dasmahapatra S and McCoy B M 1992 Spectrum and completeness of the integrable 3-state Potts model: a finite size study *Int. J. Mod. Phys.* A **7** (Suppl. 1A) 1–53

[3] Albertini G, Dasmahapatra S and McCoy B M 1992 Spectrum doubling and the extended Brillouin zone in the excitations of the three state Potts spin chain *Phys. Lett.* A **170** 397–403

[4] Alcaraz F C, Barber M N and Batchelor M T 1988 Conformal invariance, the XXZ chain and the operator content of two-dimensional critical systems *Ann. Phys.* **182** 280–343

[5] Ardonne E, Gukelberger J, Ludwig A W W, Trebst S and Troyer M 2011 Microscopic models of interacting Yang–Lee anyons *New J. Phys.* **13** 045006

[6] Balents L, Fisher M P A and Girvin S M 2002 Fractionalization in an easy-axis kagome antiferromagnet *Phys. Rev.* B **65** 224412

[7] Bazhanov V V and Reshetikhin N Yu 1989 Critical RSOS models and conformal field theory *Int. J. Mod. Phys.* A **04** 115–42

[8] Bogoliubov N M, Izergin A G and Korepin V E 1986 Critical exponents for integrable models *Nucl. Phys.* B **275** 687–705

[9] Blöte H W J, Cardy J L and Nightingale M P 1986 Conformal invariance, the central charge and universal finite-size amplitudes at criticality *Phys. Rev. Lett.* **56** 742–5

[10] Cappelli A, Itzykson C and Zuber J B 1987 Modular invariant partition functions in two dimensions *Nucl. Phys.* B **280** 445–65

[11] Cardy J L 1986 Effect of boundary conditions on the operator content of two-dimensional conformally invariant theories *Nucl. Phys.* B **275** 200–18

[12] Chari V and Pressley A 1994 *A Guide to Quantum Groups* (Cambridge: Cambridge University Press)

[13] Dancer K A, Finch P E, Isaac P S and Links J 2009 Integrable boundary conditions for a non-Abelian anyon chain with $D(D_3)$ symmetry *Nucl. Phys.* B **812** 456–69

[14] Dancer K A, Isaac P S and Links J 2006 Representations of the quantum double of finite group algebras and spectral parameter dependent solutions of the Yang–Baxter equation *J. Math. Phys.* **47** 103511

[15] de Wild Propitius M and Bais F A 1998 Discrete gauge theories *Particles and Fields* ed G Semenoff and L Vinet (*CRM Series in Mathematical Physics*) (New York: Springer) pp 353–3

[16] Di Francesco P and Zuber J B 1990 SU(N) lattice integrable models associated with graphs *Nucl. Phys.* B **338** 602–46

[17] Dijkgraaf R, Pasquier V and Roche P 1990 Quasi Hopf algebras, group cohomology and orbifold models *Nucl. Phys. (Proc. Suppl.)* **18** 60–72

[18] Essler F, Frahm H, Göhmann F, Klümper A and Korepin V E 2005 *The One-Dimensional Hubbard Model* (Cambridge: Cambridge University Press)

[19] Fateev V A and Zamolodchikov A B 1982 Self-dual solutions of the star-triangle relation in $\mathbb{Z}_N$-models *Phys. Lett.* A **92** 37–9

[20] Feiguin A, Trebst S, Ludwig A W W, Troyer M, Kitaev A Y, Wang Z and Freedman M H 2007 Interacting anyons in topological quantum liquids: the golden chain *Phys. Rev. Lett.* **98** 160409

[21] Finch P E 2011 Integrable Hamiltonians with $D(D_n)$ symmetry from the Fateev–Zamolodchikov model *J. Stat. Mech.* P04012

[22] Finch P E 2013 From spin to anyon notation: the XXZ Heisenberg model as a D_3 (or $su(2)_4$) anyon chain *J. Phys. A: Math. Theor.* **46** 055305
[23] Finch P E and Frahm H 2012 Collective states of interacting $D(D_3)$ non-Abelian anyons *J. Stat. Mech.* L05001
[24] Finch P E, Frahm H and Links J 2011 Ground-state phase diagram for a system of interacting, $D(D_3)$ non-Abelian anyons *Nucl. Phys.* B **844** 129–45
[25] Foerster A 1996 Quantum group invariant supersymmetric t–J model with periodic boundary conditions *J. Phys. A: Math. Gen.* **29** 7625–33
[26] Frahm H and Korepin V E 1990 Critical exponents for the one-dimensional Hubbard model *Phys. Rev.* B **42** 10553–65
[27] Frahm H and Yu N C 1990 Finite size effects in the integrable XXZ Heisenberg model with arbitrary spin *J. Phys. A: Math. Gen.* **23** 2115
[28] Gepner D 1992 Foundations of rational quantum field theory: I *Caltech preprint* CALT-68-1825 (arXiv:hep-th/9211100)
[29] Gepner D and Qiu Z 1987 Modular invariant partition functions for parafermionic field theories *Nucl. Phys.* B **285** 423–53
[30] Gils C, Ardonne E, Trebst S, Huse D A, Ludwig A W W, Troyer M and Wang Z 2013 Anyonic quantum spin chains: spin-1 generalizations and topological stability arXiv:1303.4290
[31] Gils C, Ardonne E, Trebst S, Ludwig A, Troyer M and Wang Z 2009 Collective states of interacting anyons, edge states and the nucleation of topological liquids *Phys. Rev. Lett.* **103** 070401
[32] Gómez C, Ruiz-Altaba M and Sierra G 1996 *Quantum Groups in Two-Dimensional Physics* (Cambridge: Cambridge University Press)
[33] Gould M D 1993 Quantum double finite group algebras and their representations *Bull. Aust. Math. Soc.* **48** 275–301
[34] Grosse H, Pallua S, Prester P and Raschhofer E 1994 On a quantum group invariant spin chain with non-local boundary conditions *J. Phys. A: Math. Gen.* **27** 4761–71
[35] Hamer C J 1981 Q-state Potts models in Hamiltonian field theory for $Qgeq4$ in $(1+1)$ dimensions *J. Phys. A: Math. Gen.* **14** 2981–3003
[36] Ikhlef Y, Jacobsen J L and Saleur H 2009 A Temperley–Lieb quantum chain with two- and three-site interactions *J. Phys. A: Math. Theor.* **42** 292002
[37] Kakashvili P and Ardonne E 2012 Integrability in anyonic quantum spin chains via a composite height model *Phys. Rev.* B **85** 115116
[38] Karowski M and Zapletal A 1994 Quantum group invariant integrable n-state vertex models with periodic boundary conditions *Nucl. Phys.* B **419** 567–88
[39] Kitaev A 2006 Anyons in an exactly solved model and beyond *Ann. Phys.* **321** 2–111
[40] Kitaev A Yu 2003 Fault-tolerant quantum computation by anyons *Ann. Phys.* **303** 2–30
[41] Kitanine N, Kozlowski K K, Maillet J M, Slavnov N A and Terras V 2011 A form factor approach to the asymptotic behavior of correlation functions in critical models *J. Stat. Mech.* P12010
[42] Korepin V E, Bogoliubov N M and Izergin A G 1993 *Quantum Inverse Scattering Method and Correlation Functions* (Cambridge: Cambridge University Press)
[43] Klümper A and Pearce P A 1992 Conformal weights of RSOS lattice models and their fusion hierarchies *Physica* A **183** 304–50
[44] Laughlin R B 1983 Anomalous quantum Hall effect: an incompressible quantum fluid with fractionally charged excitations *Phys. Rev. Lett.* **50** 1395
[45] Ludwig A W, Poilblanc D, Trebst S and Troyer M 2011 Two-dimensional quantum liquids from interacting non-Abelian anyons *New J. Phys.* **13** 045014
[46] Majid S 1995 *Foundations of Quantum Group Theory* (Cambridge: Cambridge University Press)
[47] Kedem R and McCoy B M 1993 Construction of modular branching functions from Bethe's equations in the 3-state Potts chain *J. Stat. Phys.* **71** 865–901

[48] McKay J 1980 Graphs, singularities and finite groups *The Santa Cruz Conference on Finite Groups* vol 37 (*Univ. California, Santa Cruz, CA, 1979*) pp 183–6
[49] Moessner R and Sondhi S L 2001 Resonating valence bond phase in the triangular lattice quantum dimer model *Phys. Rev. Lett.* **86** 1881
[50] Moore G and Read N 1991 Nonabelions in the fractional quantum Hall effect *Nucl. Phys.* B **360** 362–96
[51] Nayak C, Simon S H, Stern A, Freedman M and Sarma S D 2008 Non-Abelian anyons and topological quantum computation *Rev. Mod. Phys.* **80** 1083–159
[52] Pasquier V 1987 Lattice derivation of modular invariant partition functions on the torus *J. Phys. A: Math. Gen.* **20** L1229–37
[53] Pasquier V 1987 Two-dimensional critical systems labelled by Dynkin diagrams *Nucl. Phys.* B **285** 162–72
[54] Pasquier V 1988 Etiology of IRF models *Commun. Math. Phys.* **118** 355–64
[55] Roche P 1992 On the construction of integrable dilute ADE models *Phys. Lett.* B **285** 49–53
[56] Romers J 2011 private communication
[57] Sklyanin E K 1988 Boundary conditions for integrable quantum systems *J. Phys. A: Math. Gen.* **21** 2375–89
[58] Suzuki J 1988 Simple excitations in the nested Bethe-ansatz model *J. Phys. A: Math. Gen.* **21** L1175–80
[59] Trebst S, Ardonne E, Feiguin A, Huse D, Ludwig A and Troyer M 2008 Collective states of interacting Fibonacci anyons *Phys. Rev. Lett.* **101** 050401
[60] Trebst S, Troyer M, Wang Z and Ludwig A W W 2008 A short introduction to Fibonacci anyon models *Prog. Theor. Phys. Suppl.* **176** 384
[61] von Gehlen G and Rittenberg V 1986 Operator content of the three-state Potts quantum chain *J. Phys. A: Math. Gen.* **19** L625
[62] Warnaar S O and Nienhuis B 1993 Solvable lattice models labelled by Dynkin diagrams *J. Phys. A: Math. Gen.* **26** 2301–16
[63] Yang C N and Yang C P 1969 Thermodynamics of a one-dimensional system of bosons with repulsive delta-function interaction *J. Math. Phys.* **10** 1115–22
[64] Zamolodchikov A B and Fateev V A 1985 Nonlocal (parafermion) currents in two-dimensional conformal quantum field theory and self-dual critical points in Z_n-symmetric statistical systems *Sov. Phys.—JETP* **62** 215–25